LA-UR- 98-1676

Approved for public release; distribution is unlimited.

Title: THREE-BODY COLLISION CONTRIBUTIONS TO RECOMBINATION AND COLLISION-INDUCED DISSOCIATION. I. CROSS SECTIONS

CONF-9806139--

Author(s): Russell T Pack
Robert B. Walker
Brian Kendrick

Submitted to: Journal of Chemical Physics

Los Alamos
NATIONAL LABORATORY

DISCLAIMER

LA-UR-98-0000
CONF-9806139--

THREE-BODY COLLISION CONTRIBUTIONS TO RECOMBINATION AND COLLISION-INDUCED DISSOCIATION. I. CROSS SECTIONS

Russell T Pack, Robert B. Walker, and Brian K. Kendrick

Theoretical Division (T-12, MS B268), Los Alamos National Laboratory, Los Alamos, New Mexico 87545

(April 10, 1998)

Abstract

Many of the current chemical kinetics textbooks and kinetics papers treat atomic and molecular recombination and collision-induced dissociation (CID) as occurring only via sequences of two-body collisions. Actually, there is considerable evidence from experiment and classical trajectory calculations for contributions by true three-body collisions to the recombination of atomic and diatomic radicals, and that evidence is reviewed. Then, an approximate quantum method treating both two-body and three-body collisions simultaneously and on equal footing is used to calculate cross sections for the reaction $Ne_2 + H \rightleftharpoons Ne + Ne + H$. The results provide clear quantum evidence that direct three-body collisions do contribute significantly to recombination and CID.

Ms number 000000JCP. PACS numbers: 34.10.+x, 82.20.Hf, 82.30.Lp, 82.30.Nr

I. INTRODUCTION

Atomic and molecular recombination and collision-induced dissociation (CID) reactions comprise two of the most fundamental types of chemical reactions. They are important in all gas phase chemistry; for example, about half of the 196 reactions identified as important in combustion chemistry are recombination or CID reactions.[1] The overall chemical equation for any recombination reaction is the forward direction of

$$A + B + M \rightleftharpoons AB + M, \tag{1}$$

where A and B are any atoms, molecules, or radicals for which AB has bound states, and the third body M is any species that can carry away the excess energy. The overall equation for CID is simply the reverse direction of Reaction (1).

In most of the chemical kinetics literature, both textbooks and journals, recombination is assumed to proceed via two collisional mechanisms. One of these is the Lindemann energy transfer (ET) mechanism,[2]

$$A + B \rightleftharpoons AB^*, \tag{2}$$

$$AB^* + M \rightleftharpoons AB + M. \tag{3}$$

Here species with an asterisk, such as AB^*, represent metastable intermediates. The other mechanism is the bound complex (BC) mechanism (also known as the radical-molecule complex, exchange, or chaperone mechanism),[3]

$$A + M \rightleftharpoons AM^*, \tag{4}$$

$$AM^* + M \rightleftharpoons AM + M, \tag{5}$$

$$AM + B \rightleftharpoons AB + M. \tag{6}$$

An equivalent set of BC equations involving the species BM and BM^* can also contribute.

Clearly, the BC mechanism can only be important if M has enough attraction for A and/or B to produce a significant population of the AM and/or BM intermediates of the mechanism, and in the past there has been controversy[4–6] over the relative contributions of the ET and BC mechanisms. We consider that issue in future publications.[7]

The reader should note that both the ET and the BC mechanisms proceed via sequences of *two-body* collisions. In the present work, we consider the question of the role and importance of *direct three-body* (3B) collisions (or half collisions), i.e., of Reaction (1) happening directly in one step. To keep this present problem manageable, we restrict the discussion to cases in which M is sufficiently inert that the BC mechanism contributes negligibly. Then, we can directly compare the contributions of the ET and true 3B mechanisms. The present paper also emphasizes the case in which A and B are neutral, but it applies fully if one is an ion. It does not directly apply if they are oppositely charged ions, but some of the concepts are still relevant.

Before reviewing work on the 3B question, we note that, because recombination and CID are just the reverses of one another, the time-reversal invariance of quantum mechanics requires that both reactions involve exactly the same scattering matrix. As a consequence, their cross sections are directly related by microscopic reversibility, and their rate constants are related by detailed balance. Hence, if recombination proceeds only via a sequence of two-body collisions, then CID must proceed by exactly the reverse sequence of two-body collisions. Conversely, if CID can proceed directly with a significant cross section, then the rate of direct 3B recombination must also be significant.

Many early works on recombination explicitly allowed true three-body collisions by estimating the likelihood that, while a pair of atoms or molecules were in the process of colliding, a third atom or molecule would collide with them.[8] However, with only crude molecular diameters and times of simple direct collisions, these estimates were, at best, of only order-of-magnitude accuracy. Also, if one considers the intermediates AB^* in the ET mechanism to include *all* pairs regardless of their lifetimes, then in principle the ET mechanism also includes the true 3B collision contributions. Several authors[9] did that, but their

estimates were also crude. Other authors[10] used transition state theory with an unspecified mechanism to sidestep the issue of the importance of 3B collisions.

In the 1960's Smith[11] formulated a theory of recombination in which the rate is the sum of ET and direct three-body (3B) rates. In it, the ET rate depends directly on the collision lifetime of the AB^*, and Smith pointed out that it can give a negative contribution at some energies. We[12] found, in accurate calculations on Reaction (2) for the case in which A is H and B is O_2, that the negative contribution can be significant, at least for low angular momenta. Since rate constants must be positive, this negative contribution must either be unphysical, as some[13,14] have concluded, or else there must be a significant, compensating true 3B contribution to keep the total contributions positive at every energy. Until the present work, no estimates of the 3B contributions to Smith's formulation had been made that were accurate enough to answer this question.

An influential development was the 1968 "orbiting resonance theory" (ORT) of atomic recombination by Roberts, Bernstein, and Curtiss (RBC).[15,6] They assumed the ET mechanism and argued that "for most recombination reactions" the contribution of nonresonant, direct three-body collisions is "small compared to the resonance contribution." Bunker[16] had already noted that, in classical calculations, the orbiting states of AB at the top of angular momentum barriers are important. RBC noted that, when A and$B$ are atoms, their only metastable states AB^* are the resonant quasibound (QB) states trapped behind an angular momentum barrier, and they asserted that recombination is dominated by them . They assumed that these AB^* are formed by quantum tunneling through the barrier and that Reaction (2) maintains equilibrium for all contributing resonances. With those assumptions and inclusion of only the forward direction of Reaction (3) RBC were able to calculate recombination rate constants, and the initial results agreed quite well with experiment.

The RBC theory is very appealing. It provides a simple way to picture recombination reactions and allows calculations without the complexities of 3B collisions. As a result, it has had a great influence on how recombination reactions are viewed and treated. Despite the fact that more recent calculations (discussed below) have not been very successful, it contin-

ues to be used.[17] More importantly, from many discussions with colleagues, it appears to us that a majority of physical chemists now view recombination as happening via the RBC-ET mechanism. Whole books[18] are now being written on the subject of CID and recombination which do not even mention the possibility of 3B collisions. Looking at textbooks, we have found one[19] that goes so far as to assert that 3B contributions are *small*, then does a 3B estimate, gets a result *larger* than experiment, and then essentially throws that result away. Other textbooks[20] are so indefinite that readers can continue with whatever preconceptions they have, some[21] do better by giving the older[8] treatment of 3B collisions as well as the ET and BC mechanisms, and one[22] clearly attributes atomic recombination to three-body collisions but does not give a detailed treatment.

Actually, there is a considerable body of evidence that suggests that the RBC-ET mechanism is inadequate and that 3B collisions contribute, as we now discuss. As the *first* type of such evidence, we note that, not long after the advent of the RBC theory, it was discovered[23] that it predicts a very non-statistical ortho-para ratio of the H_2 formed in the recombination of H atoms. However, experiments[24] at both high and low temperatures gave statistical ortho-para ratios–in clear disagreement with the prediction. These results did not, however, change many opinions because of a possibility that rapid exchange reactions between H atoms and newly formed, highly vibrationally excited, H_2 molecules were scrambling the ortho-para ratios in the experiments.

A *second* type of evidence for 3B collision contributions comes from the pressure dependence of the reaction rates. To discuss that, we first consider the kinetics of recombination of the ET mechanism using Equations (2) and (3). Assuming the well-known steady-state approximation for the concentration of intermediates AB^* (which is more accurate than the equilibrium approximation used by RBC), one finds, neglecting the reverse of (3), that the concentration of intermediates is

$$[AB^*] = k_2[A][B]/(k_{-2} + k_3[M]), \tag{7}$$

and that the rate of formation of AB is

$$d[AB]/dt = k_{eff}[A][B], \tag{8}$$

where the effective second-order rate constant k_{eff} is

$$k_{eff} = k_2 k_3[M]/(k_{-2} + k_3[M]). \tag{9}$$

The subscripts on the rate constants refer to the numbered equations and their reverses, and the square brackets are concentrations. (Actually, the rate constant, symbolized by one term here, is a sum of such terms, one for every metastable state AB^*.) Noting that $k_{-2} = 1/\tau_2$, where τ_2 is the AB^* lifetime, one can rewrite Eq. (9) as

$$k_{eff} = K_2 k_3[M]/(1 + \tau_2 k_3[M]), \tag{10}$$

where $K_2 = k_2/k_{-2}$ is the equilibrium constant the formation of the AB^* state. At small [M] (low pressure), the denominator of Eq. (10) becomes unity, and k_{eff} is directly proportional to [M], giving pure third-order kinetics. At intermediate pressures, k_{eff} vs. [M] displays curvature known as "falloff."[25] At large [M], for all AB^* with significant lifetimes, the $AB*$ concentration of Eq. (7) decreases, the second term in the denominator in Eq. (10) dominates, and the [M] cancels causing k_{eff} to become independent of [M]. (In this regime, equivalent treatment of CID gives unimolecular kinetics.) We note at this point that direct 3B collisions via Eq. (1) give pure third-order kinetics for recombination at all pressures. The ET mechanism can only give third-order kinetics at high pressure if states AB^* with negligible lifetimes, i.e., true 3B collisions, are included.

Experimentally, for systems in which AB is a large polyatomic molecule, so that A and/or B are polyatomic molecules, k_{eff} is observed[26] to be independent of [M] and CID to be unimolecular over a large range of [M]. Hence, as shown by Klots,[27] the direct 3B contributions are negligible compared to the ET contributions for such systems, and the appropriate theory is a generalization of the ideas of RBC.[15] This is because such AB have so many long-lived vibration-rotation states lying above the dissociation energy that the rates are limited by vibrational redistribution. However, in the important case in which A and B are both atoms, k_{eff} is linear[25] to very high pressures (kbar) and only departs

from linearity because of diffusion limiting and cage (geminate recombination) effects,[28] not because of its denominator. That implies that atomic recombination is dominated by AB^* lifetimes that are too short to be RBC's quasibound states; instead, they are true 3B collisions. For cases of intermediate complexity, in which B is a diatomic and A is an atom or diatomic, the observed k_{eff} shows curvature but still rises steeply until diffusion limiting pressures are reached.[25,29] The best calculations[30] on such systems using only the ET mechanism with finite lifetime AB^* states gives a k_{eff} which is too small at high pressures. Hence, for such systems both 3B collisions and ET intermediates with significant lifetimes are making appreciable contributions. Such pressure dependence has been known for some time; as far are we know, its implications were first clearly pointed out in our preliminary account of the present work.[31] In the remainder of this paper we restrict discussion to cases in which A and B are atoms or diatomic molecules.

A *third* kind of evidence for true 3B collisions comes from classical mechanics which has often been used to study recombination and CID. Quantally, the quasibound states of the RBC theory can be formed by tunneling through the angular momentum barrier. However, classically, no tunneling is allowed, and the classical analogs of the quasibound states, the rotationally trapped states, act like bound states; they can only be formed or dissociated via true 3B collisions. Despite this fact, classical calculations of both recombination[32] and CID[33] give rates that agree very well with experiment! An excellent example is the work of Schwenke[34,35] who did a careful study of the recombination of H atoms in H_2. After constructing a new H_4 potential energy surface, he first[34] assumed the RBC mechanism, accurately calculated the tunneling rates in Eq. (2), and used classical mechanics to calculate the rates of Eq. (3). The resulting recombination rates were a factor of two to three *smaller* than experiment at all temperatures. Then, he did a second calculation[35] in which he also included the classical 3B collisional rates of formation and dissociation of both the bound and quasibound states and solved the master equations for the kinetics; the results agreed well with experiment! Furthermore, he found that omitting the tunneling rates essential to the RBC mechanism reduced the calculated rates by less than 14%. He concludes that, "at

least for the temperature range of the present study, the fundamental assumption of the ORT, namely that recombination takes place predominantly via a sequence of bimolecular collisions, is invalid. Instead we find that direct recombination due to three body collisions is the dominant pathway." Unfortunately, his study and conclusion have received too little attention.

Similar conclusions and additional information come from many detailed master equation studies of CID and recombination of H atoms.[36–39] All these included direct 3B collisional rates obtained from classical trajectory or model calculations. Pritchard and coworkers[37] found that the contribution of tunneling is negligible, the main contribution is 3B recombination, and that it is important to include both forward and reverse rates between all possible states of H_2 "in direct conflict with orbiting resonance theory (ORT)." Kung and Anderson[38] found large contributions by direct three-atom collisions. Dove and Raynor[39] found that the relative contributions of tunneling and 3B collisions depended on the pressure and that tunneling was often negligible. In a similar study of the recombination of He^+ with He, Russell and Shyu[40] found that inclusion of the quasibound states made only a 10 to 20% difference.

Clearly, it would be best to compare the RBC-ET and true 3B collision mechanisms by doing exact quantum calculations of CID and recombination. However, such calculations are difficult, and none have been reported. Authors[41] have reported exact CID calculations using 3 collinear atoms, and they found that the calculations had to be carried to large distances to separate the bound from the continuum states. They also found significant probabilities for direct 3B collisions, but, because the quasibound states of the RBC-ET mechanism do not exist in collinear calculations, such calculations cannot compare the RBC and 3B mechanisms.

In the full three-dimensional physical space, several calculations using Faddeev-type theories[42–45] have been reported. Most[42,43] were not accurate enough to address the present question. One[44] did find that true 3B collisions are required to explain the recombination of H atoms in He at extremely low temperatures, and one[45] is approaching the accuracy

needed for applications to the present question. Also, a recent calculation for the CID of H_2 by Ar appeared[46], which found direct dissociation, but the distorted-wave-Born approximation used is too crude for present use; the potential is involved to high orders in the CID process.

Miller[13] has proposed a flux-flux correlation function theory for recombination which includes AB^* of *all* lifetimes, so that it includes both the RBC and 3B mechanisms, and it has been applied to $H + O_2$ recombination.[14] However, in its present form, an integral part of the theory is the strong collision approximation which assumes that every intermediate AB^* is deexcited to a bound AB on every collision with an M. That approximation is so crude that it severely limits the ability of the theory to address the present question. (Future improvements[47] may overcome this limitation.) Nonetheless, in their application of the present version of Miller's theory to $H + CO$ recombination, Qi and Bowman[48] saw evidence of nonresonant (true 3B) contributions at high temperatures. At low temperatures, this particular recombination is dominated by resonances because, for all angular momenta, there is a barrier in the potential energy surface (PES) and only the resonant states can get close enough together to recombine.

Although the large distances required will make the calculations difficult, we expect that exact 3D quantum calculations of recombination and CID for 3 atom systems will soon begin appearing. Some of the new methods currently in use in rearrangement scattering should be applicable, and we[7] are working on the problem using hyperspherical methods.[49]

The one previous work that has the same purpose as the present work [*i.e.*, to compare the contributions of resonant (successive two-body) and nonresonant (true three-body) collisions] is that of Pan and Bowman[50] on the CID of HCO by Ar. To make a quantum treatment of this difficult four-body problem tractable, they used sudden approximations on several variables, averaged the potential over one angle, and used L^2 vibrational functions to discretize the continuum. They find both resonant and 3B contributions with the resonant contributions dominating. However, part of this result could be due to the aforementioned barrier in the HCO PES. Barrierless systems may be less resonant-dominated.

Another approximate method that should be mentioned is that of Nobusada and Sakimoto.[51] They studied the CID of H_2 by He, treating rotation with the familiar[52] Rotationally Infinite Order Sudden (RIOS) approximation and the two remaining coordinates via a hyperspherical coupled channel (CC) method. Unfortunately, they introduce walls at large distances to discretize the continuum in the very region where we want to compare the roles of the quasibound and continuum states, so their method cannot be used to answer the present question.

In the present work, a brief account of which has already appeared,[31] we report approximate calculations of CID aimed at comparing the contributions of the sequential two-body mechanisms of the RBC-ET type with those of true three-body (3B) collisions. We consider three-atom systems and use the VRIOS approximation of Pfeffer[53], in which both the Vibrational and Rotational motions are treated in the IOS approximation. While this approximation is very simple, it has the advantage of exactly conserving probability and of treating all the bound, quasibound, and continuum states of the diatomic simultaneously and on equal footing, making it easy to compare their contributions. Sakimoto[54] has also reported VRIOS calculations of CID. However, he only calculated the total dissociation cross section; the present problem requires more detail.

In the next Section we review the VRIOS approximation and give the formulas needed for calculations. Then, in Section III we describe our calculations and report the results for the CID of Ne_2 by H atoms. Section IV contains our conclusions. The present paper reports the calculated integral cross sections; in the following paper[55] rate constants are calculated from those cross sections, and the kinetics of CID and recombination for this system are studied using a master equation approach.

II. THEORY

In this section we consider a system composed of three atoms, A, B, and M, and outline an approximation in which both the vibrational and rotational motions of AB are treated

in the infinite order sudden approximation. When those vibrational or rotational levels are widely spaced in energy, the resulting VRIOS approximation will be crude except at high energies; however, when they are closely spaced, it, like the familiar RIOSA, is expected to give qualitative to semiquantitative accuracy, and it has two particular advantages: It exactly conserves probability, and it treats the bound and continuum states of AB simultaneously and on the same footing.

A. Formulation

We use the set of Jacobi coordinates in which $\mathbf{r}$ is the vector from A to B, $\mathbf{R}$ is the vector from the center of mass of AB to M, and γ is the angle between $\mathbf{r}$ and $\mathbf{R}$. We only need the coordinates for this one arrangement. As Wei, Alavi, and Snider[56] have pointed out, one gets the complete answer using only one arrangement if the calculations are carried out exactly, and one must be careful to avoid double counting if more than one arrangement is used. In practice, describing the bound and quasibound states of AM and BM accurately using only the present coordinates would be very difficult. However, as explained in the Introduction, this discussion is restricted to systems in which the bound and quasibound states of AM and BM and hence the BC mechanism contribute negligibly.

We now summarize a derivation of the VRIOS[53] approximation that is applicable to situations in which all three atoms may be unbound using notation similar to our earlier RIOS[52] work, so that many of the same formulas may be used. It is assumed that the scattering takes place on a single, nondegenerate potential energy surface (PES). The objective is to solve the Schrödinger equation,

$$(E - H)\Psi = 0. \tag{11}$$

The Hamiltonian here is

$$H = -\frac{\hbar^2}{2\mu_{M-AB}R}\frac{\partial^2}{\partial R^2}R + \frac{\mathbf{L}^2}{2\mu_{M-AB}R^2} + H_{AB} + V(R, r, \gamma), \tag{12}$$

where H_{AB} is the Hamiltonian of an isolated AB subsystem,

$$H_{AB} = -\frac{\hbar^2}{2\mu_{AB}r}\frac{\partial^2}{\partial r^2}r + \frac{\mathbf{J}_{AB}^2}{2\mu_{AB}r^2} + v(r). \tag{13}$$

Here v is the AB interatomic potential, and V is the rest of the PES, so that the total PES is $V+v$. μ_{M-AB} is the $M-AB$ reduced mass, μ_{AB} is the AB reduced mass, $\mathbf{J}_{AB}$ is the AB angular momentum, and $\mathbf{L}$ is the orbital angular momentum of M relative to AB.

We use space-frame coordinates and couple the rotational wavefunctions via the Clebsch-Gordan theorem in the usual way[52] to form eigenfunctions $|jlJM>$ of the total angular momentum. We also use the complete set of eigenfunctions $\chi_{\nu j}(r)$ for the radial motion of AB, satisfying

$$[-\frac{\hbar^2}{2\mu_{AB}r}\frac{\partial^2}{\partial r^2}r + \frac{\hbar^2 j(j+1)}{2\mu_{AB}r^2} + v(r) - \epsilon_{\nu j}]\chi_{\nu j}(r) = 0. \tag{14}$$

Here the index ν is discrete for the bound states but continuous for the AB scattering states. The χ are normalized to unity for the bound states and normalized to a delta function on the wavenumber of the AB relative motion, $\kappa = (2\mu_{AB}\epsilon_{\nu j}/\hbar^2)^{\frac{1}{2}}$, for the continuum states.

We expand the total wavefunction Ψ for total angular momentum J in the complete set of products as

$$\Psi^i = \sum_n (Rr)^{-1} G^J_{ni}(R)\chi_{\nu_n j_n}(r)|j_n l_n JM>, \tag{15}$$

where $n = (\nu_n, j_n, l_n)$ is a composite index, and i is the composite index of the incident state. The sum here includes an integral over all the continuum states of AB. Substituting this into Eq.(11) and projecting with state f gives,

$$[\frac{d^2}{dR^2} + k_f^2 - \frac{l_f(l_f+1)}{R^2}]G^J_{fi}(R) = \frac{2\mu_{M-AB}}{\hbar^2}\sum_n < \nu_f j_f l_f J|V|\nu_n j_n l_n J > G^J_{ni}(R), \tag{16}$$

where $k_f^2 = \frac{2\mu_{M-AB}}{\hbar^2}(E - \epsilon_{\nu_f j_f})$. The index M is suppressed here because the equations are independent of M. Although these look just like the familiar coupled channel (CC) equations, they cannot be directly solved by standard (matrix) numerical methods because of the uncountably infinite set of continuum states coupled together. Direct solution would require use of the techniques mentioned in the Introduction.

The VRIOS approximation proceeds as follows. We replace two operators in Eq. (12) by eigenvalue forms; namely,

$$\mathbf{L}^2 \approx \hbar^2 \bar{l}(\bar{l}+1), \tag{17}$$

and

$$H_{BC} \approx \bar{\epsilon}. \tag{18}$$

That replaces Equation (11) by

$$(E - \bar{H})\Gamma^{\bar{k}\bar{l}}(R; r, \gamma) = 0, \tag{19}$$

or, with $\Gamma = g/R$,

$$[\frac{d^2}{dR^2} + \bar{k}^2 - \frac{\bar{l}(\bar{l}+1)}{R^2} - \frac{2\mu_{M-AB}}{\hbar^2} V(R, r, \gamma)] g^{\bar{k}\bar{l}}(R; r, \gamma) = 0, \tag{20}$$

where $\bar{k}^2 = \frac{2\mu_{M-AB}}{\hbar^2}(E - \bar{\epsilon})$. Now, Eq. (20) is a single, uncoupled equation, and r and γ have become parameters. For any given values of them, the equation can be solved subject to usual scattering boundary conditions to generate phase shifts $\eta_{\bar{l}}^{\bar{k}}(r, \gamma)$. (We note that $R >> r$ is required to apply the asymptotic boundary conditions.) From the phase shifts one constructs parameter-dependent Scattering and Transition matrices as

$$\mathcal{S}^{\bar{k}\bar{l}}(r, \gamma) = \exp[2i\eta_{\bar{l}}^{\bar{k}}(r, \gamma)] \tag{21}$$

amd

$$\mathcal{T}^{\bar{k}\bar{l}}(r, \gamma) = 1 - \mathcal{S}^{\bar{k}\bar{l}}(r, \gamma). \tag{22}$$

With this, one finds that, as is familiar from the RIOS[52] approximation, the matrix element,

$$\tilde{G}^J_{f_i}(R) = i^{l_i - \bar{l}} < \nu_f j_f l_f JM | g^{\bar{k}\bar{l}}(R; r, \gamma) | \nu_i j_i l_i JM >, \tag{23}$$

is an approximate solution of the complete, continuous, infinite set of CC equations. To demonstrate that, one takes this matrix element of Eq. (20), inserts closure, and obtains

$$[\frac{d^2}{dR^2} + \bar{k}^2 - \frac{\bar{l}(\bar{l}+1)}{R^2}]\tilde{G}^J_{fi}(R) = \frac{2\mu_{M-AB}}{\hbar^2}\sum_n < \nu_f j_f l_f J|V|\nu_n j_n l_n J > \tilde{G}^J_{ni}(R), \qquad (24)$$

which is the complete set of CC equations with the two obvious approximations. The VRIOS approximation to the physical Transition matrix is

$$\tilde{T}^J(\nu_f j_f l_f|\nu_i, j_i, l_i) = i^{l_f+l_i-2\bar{l}} < \nu_f j_f l_f JM|\mathcal{T}^{\bar{k}\bar{l}}(r,\gamma)|\nu_i j_i l_i JM > . \qquad (25)$$

All desired scattering properties can be calculated from this transition matrix.

B. Cross Sections

We note that, in the VRIOSA as in the RIOSA, many simplifications occur in the calculation of scattering amplitudes, differential cross sections, integral cross sections, and total cross sections. For this paper our interest is in integral and total cross sections, and we only give the formulas for those. More detailed derivations are in our earlier paper.[52]

It is computationally convenient, after calculating the $\mathcal{T}^{\bar{k}\bar{l}}(r,\gamma)$ at an array of r and γ points, to calculate the following:

$$\mathcal{T}^{\bar{k}\bar{l}}_{fi}(\gamma) =< \chi_{\nu_f j_f}|\mathcal{T}^{\bar{k}\bar{l}}(r,\gamma)|\chi_{\nu_i j_i} >, \qquad (26)$$

where now $f = (\nu_f, j_f)$, etc. These integrals over r are well defined if at least one of the χ is square integrable (bound). To be able to use the standard formulas, we carry out the calculations for both bound and continuum $\chi_{\nu_f j_f}$ but only for bound $\chi_{\nu_i j_i}$. Then, when $\bar{l}$ is chosen to be l_f, the degeneracy-averaged integral cross section formula reduces to[52]

$$\sigma(\nu_f j_f \leftarrow \nu_i j_i) = (\pi/k_i^2)\sum_{\bar{l}}(2\bar{l}+1)\mathcal{P}_{\bar{l}}(\nu_f j_f \leftarrow \nu_i j_i) \qquad (27)$$

where the opacities are given by

$$\mathcal{P}_{\bar{l}}(\nu_f j_f \leftarrow \nu_i j_i) = \frac{1}{2j_i+1}\sum_{m_i}| < j_f m_i|\mathcal{T}^{\bar{k}\bar{l}}_{fi}(\gamma)|j_i m_i >_{BF} |^2. \qquad (28)$$

We note that because the $\chi_{\nu j}$ (and hence the indexes f and i) depend on j as well as ν, one does not get the full factorization of the rigid rotor RIOSA[52] in which all cross sections can

be calculated from those for $j_i = 0$. However, these matrix elements are diagonal in m_i and are carried out in a body-frame where γ is the first angle of the spherical harmonic functions involved, so they are still simple. It is convenient make a Legendre polynomial expansion of $\mathcal{T}_{fi}^{\bar{k}\bar{l}}$ as

$$\mathcal{T}_{fi}^{\bar{k}\bar{l}}(\gamma) = \sum_L t_{fi}^{\bar{k}\bar{l}L} P_L(\cos\gamma), \tag{29}$$

where

$$t_{fi}^{\bar{k}\bar{l}L} = (L + \frac{1}{2}) \int_{-1}^{1} \mathcal{T}_{fi}^{\bar{k}\bar{l}}(\gamma) P_L(\cos\gamma) d\cos\gamma. \tag{30}$$

These are simply evaluated via one-dimensional Gauss-Legendre quadrature. Then, substitution of Eq.(29) into Eq.(28) gives the opacities as

$$\mathcal{P}_{\bar{l}}(\nu_f j_f \leftarrow \nu_i j_i) = \sum_L (2L+1)^{-1} C(j_f L j_i; 000)^2 |t_{fi}^{\bar{k}\bar{l}L}|^2, \tag{31}$$

so that all cross sections are easily calculated from the t matrices. In calculating the cross sections, we use $\bar{k} = k_i$.

The total integral cross section similarly simplifies. If one sums and integrates Eq.(27) over all final states and uses the completeness relation and the spherical harmonic addition theorem, one obtains[52]

$$\sigma_{tot}(\nu_i j_i) = < \chi_{\nu_i j_i}(r) | \sigma_{tot}(r) | \chi_{\nu_i j_i}(r) > \tag{32}$$

for the total cross section out of any given initial state, where

$$\sigma_{tot}(r) = \frac{1}{2} \int_{-1}^{1} \sigma(r,\gamma) d\cos\gamma, \tag{33}$$

and where

$$\sigma(r,\gamma) = (\frac{4\pi}{k_i^2}) \sum_{\bar{l}} (2\bar{l}+1) \sin^2[\eta_{\bar{l}}^{\bar{k}}(r,\gamma)]. \tag{34}$$

This last equation is the simple integral cross section formula for the scattering of spherical particles. This simple, alternate way to calculate $\sigma_{tot}(\nu_i j_i)$ is a direct result of the fact that

the VRIOSA, like the RIOSA, exactly conserves probability, and it is very useful in the present problem because it allows testing the completeness of the bound and continuous basis used by comparing the σ_{tot} of Eq. (32) with the numerical result of summing and integrating $\sigma(\nu_f j_f \leftarrow \nu_i j_i)$ over all final states in the basis.

We note at this point that if the initial and final vibrational states are both bound states, the $\sigma(\nu_f j_f \leftarrow \nu_i j_i)$ from Eq. (27) have the usual state to state integral cross section interpretation, but if the final state is a continuum state of AB, then the cross section calculated via this formula is really differential in κ, and might better be written as $d\sigma/d\kappa$ for the transition. Integration of it over κ yields the bound-free integral cross section via

$$\sigma(j_f \leftarrow \nu_i j_i) = \int \sigma(\nu_f j_f \leftarrow \nu_i j_i) d\kappa. \tag{35}$$

If the integration range chosen here is $(0, \infty)$, on obtains the bound-free integral cross section, but one can also choose to integrate only over shorter intervals to pick out the contributions of particular resonances or certain relative energy regions.

III. CALCULATIONS AND RESULTS

A. System and Potential Energy Surface

The specific system studied in this work was

$$Ne_2 + H \rightleftharpoons Ne + Ne + H, \tag{36}$$

that is, $A = B = Ne$ and $M = H$. While it would admittedly be difficult to study experimentally, it is a real system, and it is simple enough to allow detailed calculations to be carried out and analyzed. As will be shown in the following paper[55], results for this system are more applicable to systems containing strongly binding atoms than one might at first think. Although Ne_2 lacks the deeply bound states of a chemically bound molecule, all evidence suggests that such deeply bound states are accessed only by vibrotational relaxation

anyway. The processes that are key in this system must also happen among the highly excited states of chemically bound molecules in their CID and recombination.

H atoms were chosen as the third body because the NeH potential well is so shallow that it has no bound or quasibound states. That means that the BC mechanism is rigorously excluded from contributing, and the only two mechanisms possible are the ET and 3B mechanisms. This clarifies the interpretation of the results and allows a direct comparison of the two mechanisms.

The isotope ^{18}Ne was chosen for the present calculations because it was found that, for the more common isotope, the diatom $^{20}Ne_2$ is extraordinary (and somewhat similar to $^4He_2$) in having a state (v,j)=(2,0) bound by only 0.032 Kelvin[57] whose wavefunction extends to such large distances and couples so well to the 3B continuum as to make it less representative of a typical diatomic and thus make any conclusions less general. (For weakly bound systems it is convenient to measure energies in Kelvin (K), so that energies are really E/k_B, where k_B is Boltzmann's constant.)

We note that the physical picture of the CID or recombination process provided by the VRIOSA is that, while two Ne atoms are interacting, an H atom comes rapidly past, collides with them, and causes a transition. In this time-independent formulation, no time sequence is implied, and the Ne atoms can be at any distance and in any stage of a bound vibration or a $Ne-Ne$ collision when the H collides with them. The levels of $^{18}Ne_2$ are rather closely spaced, and the sudden approximation is expected to be valid for transitions such that[58] $\Delta\epsilon \ll \hbar/\tau$, where $\Delta\epsilon$ is the change in the relative energy of the $Ne-Ne$ pair, and τ is the lifetime of the $H-Ne_2$ collision. At the energies (~30K) of primary interest, τ is about 0.3 psec, which gives the sudden condition as $\Delta\epsilon \ll 27$ K. As it turns out in the calculations and results discussed later in this paper, this condition is well satisfied for all the transitions that have large enough cross sections to be important to the kinetics. Hence, we expect the results to be fully semiquantitatively accurate; *i.e.*, based on previous experience, we expect the larger cross sections and the resulting kinetics to be accurate to within about 20%.

All the interactions in the Ne_2H system are weak van der Waals interactions with shallow

attractive wells. For such systems at the low energies of interest here, Meath and Aziz[59] have shown that the non-additive three-body terms in the PES largely cancel each other and contribute only a few percent of the PES. Consequently, we have taken the PES for this system to be the pairwise additive sum of interatomic potentials and used the best semi-empirical potentials available; it should have more than enough accuracy to answer the question at hand.

For the $Ne - Ne$ interaction, we used the Aziz-Slaman[57] potential, which has a well depth of 42.25 K. It was generated directly from a routine kindly sent us by them.

For the $Ne - H$ interaction, we used a potential due to Tang and Toennies.[60] Using the parameters in their paper, the best agreement with their table was obtained by truncating their sum at $2n = 16$, and this gave a well depth of 17.29 K. To avoid its divergences at small r, their potential was replaced at distances less than $0.5a_0$ by a simple repulsive exponential potential, $v = A\exp(-br)$, with, in atomic units, $A = 11.7125866$ and $b = 1.887834483$. We carefully checked both the behavior of the nodes of the NeH wavefunctions and the zero-energy phase shift[61] and confirmed that the NeH has no bound states and no quasibound states.

B. $Ne - Ne$ States

All the states of $^{18}Ne_2$ were accurately calculated numerically. The energies and wavefunctions were calculated with the renormalized Numerov method,[62] and the lifetimes (time delays) were directly calculated with the log derivative method.[62,63] The properties of all 18 long-lived states are shown in Table I; there are 8 bound states, 3 quasibound (QB) states trapped behind angular momentum barriers, 5 broad above barrier (BAB) resonances, and two barrier slowing (BS) resonances caused by slowing due to a broad low barrier. Only even j's occur because ^{18}Ne atoms are spinless bosons. As shown in the table, the e-folding lifetime of the resonances, τ_e, is one-fourth the maximum lifetime, τ_{max}, and their width is $\Gamma = \hbar/\tau_e$.[64]

Plots of a few of the Ne_2 wavefunctions are in Figures 1 and 2. In Fig. 1(a) are the two bound states for $j = 2$ and the resonant scattering state. One sees that the amplitude of the resonant state is small inside the well region; the large resonant amplitude of the wavefunction occurs atop and outside the low centrifugal barrier at this j. Hence, this is not a quasibound state but seems to be a growth of amplitude due to the slowing by the barrier. We note that the energy of the resonance (0.12 K) and of the barrier maximum (0.12 K at $r = 18.3a_0$) is so small that it can hardly be distinguished from zero (the dotted line) on the plot. Fig. 1(b) is a plot of wavefunctions for $j = 6$. The maximum lifetime of the quasibound (1,6) resonant state occurs at an energy of 1.98 K which is well within its width (0.39 K) of the barrier maximum of 2.07 K. As a result, the maximum amplitude of the wavefunction occurs just inside the barrier, and that amplitude is only a factor of two larger than the amplitude outside the barrier. The wavefunctions of both the narrow and broad resonances for $j = 10$ were plotted in a previous paper[31] and are not repeated here. Fig. 1(c) is a plot of a wavefunction near the center of the $j = 14$ broad above barrier (BAB) resonance. This is the longest lived of the BAB resonances; one sees that the amplitude in the well region is again only a factor of two larger than the asymptotic amplitude–there is little localization.

Figure 2 is a 3D perspective of the Ne_2 scattering wavefunctions for $j = 12$ as a function of energy as well as distance. It allows one to see clearly the amplitude of the wavefunction in the well region as a function of energy, and the resonant quasibound $j = 12$ state stands out clearly.

In studying the resonances it is also instructive to plot the collision lifetime or time delay versus energy. Such plots for $j = 2$ and for both the narrow and broad $j = 10$ resonances were presented in our previous paper;[31] that for $j = 4$ is shown in Fig. 3. One sees a fairly narrow peak in τ at low energies. This BS resonance, like that for $j = 2$, is simply caused by slowing due to the broad barrier; the wavefunction (not shown) at small r is always small. Note that at larger energies τ is negative over a large energy range. τ is the difference[11] between the total lifetime of the interaction and the time τ_{pass} it would take for

the two atoms to pass each other if the interaction potential were zero, and these negative, nonresonant regions mean that at these energies the collision is taking less time than it would if there were no interaction at all. We remark that for $j = 0$ there are no resonances; τ is negative at all energies.

To understand how "resonant" a resonance is, it is useful to estimate the zero interaction passage time τ_{pass} at the same energy and angular momentum. Because the tail of the van der Waals potential extends out to infinity, τ_{pass} is not uniquely defined, but it can be estimated as the time it takes noninteracting atoms to cover the distance where the interaction is large enough to be significant. From classical or semiclassical phase integrals,[11] the time two noninteracting atoms spend within a distance r_i of each other is

$$\tau_{pass} = 2(r_i^2 - b^2)^{\frac{1}{2}}/v_a \tag{37}$$

where $b = \hbar(j+\frac{1}{2})/(2\mu_{AB}\epsilon)^{\frac{1}{2}}$ is the impact parameter and $v_a = (2\epsilon/\mu_{AB})^{\frac{1}{2}}$ is the asymptotic relative velocity. To be definite we choose r_i to be the larger of $b + 0.2a_0$ and the distance at which the τ with the interaction turned on has accumulated 0.99 of its total value. The resulting values of τ_{pass} are in the last column of Table I. One sees that they vary quite a bit with energy and angular momentum. One also sees that, for most of the resonances, τ_e, which represents the average lifetime of the resonance, is less than τ_{pass}, so that the total lifetime of the interaction does not even double the passage time with no interaction. The only exceptions to this are the three quasibound (QB) states; their average lifetimes run from larger to much larger than τ_{pass}.

C. $H + Ne_2$ Scattering

The second part of the calculation is the VRIOS determination of the $H + Ne_2$ cross sections. The relative collision energy was chosen to be $E/k_B = 30K$. This is the most probable collision energy at a temperature of 30 K, where physically one can get a significant concentration of Ne_2 dimers. The phase shifts $\eta_l^E(r,\gamma)$ were calculated accurately using the

log derivative method[62] and propagating R from 0 to 40 bohr. They were calculated (using symmetry) at 50 of the points of a 100 point Gaussian quadrature in γ, at 81 values of r ranging from 3.5 to 20 bohr, and all partial waves $\bar{l}$ from 0 through 20. The radial integrals in Eqs. (26) and (32) were performed using Simpson's rule quadratures and the angular integrals of Eq. (30) and (33) by Gaussian quadratures. The calculations are converged with respect to all parameters, and they are not expensive; it requires less than 12 minutes on a HP 735 workstation to calculate all the cross sections at this energy.

Some of the resulting $d\sigma/d\kappa$ are plotted versus κ in Figure 4 for transitions from all the bound states into the continuum. κ is the wavenumber for the final relative $Ne-Ne$ motion in atomic units. To make connection to the other figures easier, we note that $\epsilon(K) = 9.62409\kappa(a_0^{-1})^2$. Thus, $\kappa = 0.1$ corresponds to $\epsilon = 0.1$, $\kappa = 0.5$ to $\epsilon = 2.4$, $\kappa = 1.0$ to $\epsilon = 9.6$, $\kappa = 2.0$ to $\epsilon = 38.5$, etc. One sees from Fig. 4(a) that several of the bound states have significant cross sections connecting them to the $j_f = 0$ continuum. Because Ne_2 has no resonances with $j_f = 0$ and because these $d\sigma/d\kappa$ spread over essentially all the energy available, these represent direct transitions to the nonresonant three-body continuum. As was shown with figures in an earlier paper,[31] the transitions to $j_f = 2$ also involve direct, non-resonant three-body collisions. The $d\sigma/d\kappa$ for $j_f = 4$ are shown in Fig. 4(b); these are also due to nonresonant, direct three-body collisions; the peaks are broad, and their maxima correspond to a $Ne-Ne$ relative energy of about 2 K which is much larger than the 0.48 K where the lifetime shows a resonant maximum. For higher j_f, resonant collisions contribute more, but there is always a contributing broad nonresonant peak; it simply becomes more difficult to see on the plots because their scales change to include the maxima of the narrow peaks. For $j_f = 6$ the sharp maximum in Fig. 4(c) is due to the quasibound (QB) (1,6) resonance, but the nonresonant peak extending to higher energies is also clearly visible. The contribution for $j_f = 8$ in Fig. 4(d) is mostly due to its broad above barrier (BAB) resonance. As shown in our earlier paper,[31] contributions for $j_f = 10$ come from its narrow QB state and its BAB resonance. The contributions for $j_f = 12$ in Fig. 4(e) are due to its QB (0,12) resonance and a nonresonant tail. The contributions for all the higher j_f shown

come from BAB resonances and nonresonant tails, and get broad and very small by the highest j_f shown. We note that the small j_f continuum states have their largest connections to the bound states that are vibrationally excited but have small j_i. For higher j_f that slowly changes until the largest connections are to bound states which have the largest j_i but have $\nu_i = 0$.

We note from the parts of Fig. (4) that it is precisely at the energies where τ is negative that $d\sigma/d\kappa$ shows the broad positive contributions from true 3B collisions. This is exactly in accord with the predictions of Smith.[11] Hence, it appears incorrect to label Smith's theory as "unphysical."[13,14] However, if one were to do calculations using Smith's theory directly, he would need to be careful to avoid undercounting or the problems of double counting that Wei, Alavi, and Snider[56] discuss. Our present formulation has no such problems; contributions are counted once and only once; we only make separations to interpret mechanisms.

We note that, because the VRIOS approximation does not contain energy thresholds, these plots extend to higher κ than would be allowed by energy conservation. However, for most of the plots, only a small and unimportant tail extends above the allowed energy. The only exceptions to that are the plots for high j_f where the whole integral over κ gives a relatively small contribution.

As can be seen from the parts of Fig. (4) the grid in κ was varied from fine to coarse as needed to describe the various narrow resonances as well as the broad peaks. That made it convenient to perform the integrals of the $d\sigma/d\kappa$ over κ to get the bound-free integral cross sections of Eq. (35) via simple trapezoidal rule quadrature. In this process, it was observed that the contributions of the narrow quasibound resonances approach δ function behavior. As the resonance narrows, the maximum in $d\sigma/dk$ gets larger and larger, but its integral over k approaches a constant. To see if it approaches the contribution of a bound state, calculations were done in which the very narrow (0,10) quasibound resonance wavefunction was replaced by a square-integrable (L^2) wavefunction which is proportional to the QB wavefunction out to its first node, zero thereafter, and normalized to unity. The results are compared in Table II, and one sees that, to the accuracy with which the continuum

quadrature was done, they are identical. Hence, the contributions of this narrow resonance can be obtained either by integration over its continuum (scattering) wavefunctions or by simply approximating it as a bound state.

The observation of the preceding paragraph is useful because it allows the contributions of the quasibound states to be approximately separated from BAB and direct three- body contributions in the cases [(1,6) and (0,12)] where the contributions are not so easily distinguished as they are for (0,10). Accordingly, that was done with square-integrable (L^2) wavefunctions which were taken proportional to their QB wavefunction out to the first node for the (0,12) state and to the second node for the (1,6) state, zero thereafter, and normalized to unity. Results using them were subtracted from the total for that j_f. Representation of the QB states by L^2 functions also then allows calculation of the cross sections for transitions from these QB states into the bound states, the other QB states, and the BAB and nonresonant continuum states.

We note that representation by an L^2 function is an excellent approximation for the (0,10), a good approximation for the (0,12), and a fair approximation for the (1,6) QB resonances; i.e., the approximation degrades as the resonances get wider. We have also tested the L^2 representation of the BAB resonances, such as that for $j = 14$, and found it to give unsatisfactory results because their wavefunctions are less localized, and the results also depend on how many nodes one includes before truncating and normalizing. This is not well defined for the BAB resonances, but it is for the QB resonances which are continuations of bound state wavefunctions. As a result, we treat the BAB resonances as part of the 3B continuum. Hence, while in principle the BAB resonances and the nonresonant continuum states can be included in the ET mechanism, in practice they cannot be included in any accurate quantum calculations of the ET mechanism; one must have L^2 representations of all the resonances used in order to carry out calculations of the second step of the process.

The resulting integral cross sections are shown in Table III. The columns are labeled by the initial states, the rows by the final states. The last three columns are cross sections out of the square integrable approximations of the QB states. Looking at the upper left 8 by 8

matrix, one sees that the bound-bound cross sections have the physically expected behavior: Vibrationally inelastic cross sections are small, and the rotationally inelastic cross sections are largest for small Δj transitions (those for which the sudden criterion is well satisfied). Lines 8 through 11 are cross sections for transitions between the bound and the QB states. They are about the same size as the bound-bound cross sections. Then, lines 12 through 22 are cross sections for transitions to all the continuum states labelled by $j_f = 0, 2, ...20$ except the QB states. Again, they are about the same size and show about the same pattern as the bound-bound cross sections. It should be noted that the QB states have large collisional cross sections connecting them to the continuum states. Finally, the cross sections to the nonresonant true three-body continuum, such as states with $j_f = 0$, 2, and 4 are very nearly as large as those to the BAB and QB resonances. We note in passing that integral cross sections from a high-lying bound state or a QB state to the continuum of a given j_f are very much the size expected for a rotationally inelastic cross section to the state if it were a bound state; this confirms the QCT and model-based choices made in many master equation studies.[36–39]

These observations are clarified by Table IV. There, the sums of cross sections for transitions of a particular type from each of the bound states are presented; namely, the rows are elastic, total bound-bound inelastic, total bound-quasibound, total bound-broad above barrier, and total bound-direct three-body continuum. For the bound states that have significant cross sections to unbound states, it is clear that all three of these categories of unbound states are important; none can be omitted.

The last two lines of Table IV are a check on the numerical calculations. The upper line is the sum of its column of Table IV (or Table III). The lower is the total integral cross section evaluated accurately using Eq. (32). Their very good agreement verifies the accuracy of our numerical calculations and the completeness of the set of bound and continuum states used in the state to state calculations; *i.e.*, they show that neither undercounting nor overcounting has occurred.

In preparation for the work reported in the following paper,[55] the calculations reported

herein were repeated at 14 energies logarithmically spaced from 3.7 to 887 K. In these, the maximum $\bar{l}$ varied from 16 to 45, the maximum j_f was 28, and the maximum κ was 6. At energies above 200K the phase shifts were calculated efficiently by quadrature of the WKB formula.[65] These choices assure good convergence of the cross sections.

IV. CONCLUSIONS

In this paper we have presented cross sections that are relevant to recombination and collision-induced dissociation (CID) for a simple reaction (36) using a simple VRIOS approximation which should be semiquantitatively accurate for it, which treats all the bound and continuum states on an equal footing and which should not favor any type of state.

The resulting cross sections show clearly that *three* types of continuum states contribute significantly to the reaction; namely, quasibound (QB) states, broad above barrier (BAB) resonances, and true nonresonant three-body (3B) continuum states. All three types contribute significantly to the reaction and must be included in treatments of the kinetics as we show in the following paper.[55]

The present results constitute clear quantum mechanical evidence that nonresonant, direct three-body collisions contribute significantly to recombination and CID, at least in simple systems.

V. ACKNOWLEDGEMENT

This work was performed under the auspices of the US Department of Energy under the Laboratory Directed Research and Development Program.

REFERENCES

[1] D. L. Baulch, et al., J. Phys. Chem. Ref. Data **21**, 411 (1992).

[2] F. A. Lindemann, Trans. Faraday Soc. **17**, 598 (1922). See also C. N. Hinshelwood, Proc. Roy. Soc. **A113**, 230 (1927).

[3] G. E. Kimball, J. Am. Chem. Soc. **54**, 2396 (1932).

[4] See, for example, G. Porter, Disc. Faraday Soc. **33**, 198 (1962) and M. Eusuf and K. J. Laidler, Trans. Faraday Soc. **59**, 2750 (1963).

[5] R. T Pack, R. L. Snow, and W. D. Smith, J. Chem. Phys. **56**, 926 (1972).

[6] P. A. Whitlock, J. T. Muckerman, and R. E. Roberts, J. Chem. Phys. **60**, 3658 (1974).

[7] B. K. Kendrick, R. B. Walker, and R. T Pack (unpublished work).

[8] R. C. Tolman, *Statistical Mechanics with Applications* (Chemical Catalog Co., New York, 1927), p. 245; L. S. Kassel, *Kinetics of Homogeneous Gas Reactions* (Chemical Catalog Co., New York, 1932) pp. 76-8; A. A. Frost and R. G. Pearson, *Kinetics and Mechanism* 2nd ed. (Wiley, New York, 1961), pp. 68-9; S. W. Benson, *The Foundations of Chemical Kinetics* (McGraw-Hill, New York, 1960), pp. 306-8; E. A. Moelwyn-Hughes, *Physical Chemistry* 2nd ed. (Macmillan, New York, 1961), p. 53; M. L. Goldberger and K. M. Watson, *Collision Theory* (Wiley, New York, 1964), p. 868.

[9] E. Rabinowitch, Trans. Faraday Soc. **33**, 283 (1937); S. W. Benson and T. Fueno, J. Chem. Phys. **36**, 1597 (1962); I Amdur and G. G. Hammes, *Chemical Kinetics* (McGraw-Hill, New York, 1966), pp. 41-3 and 200-202; H. S. Johnston, *Gas Phase Reaction Rate Theory* (Ronald Press, New York, 1966), pp. 253-262; S. W. Benson, *Thermochemical Kinetics*, 2nd ed. (Wiley, New York, 1976).

[10] K. J. Laidler, *Chemical Kinetics* 2nd ed. (McGraw-Hill, New York, 1965), pp. 137-40.

[11] F. T. Smith, in *Kinetic Processes in Gases and Plasmas*, A. R. Hochstim, ed., (Academic

Press, New York, 1969), pp. 321-381; F. T. Smith, Disc. Faraday Soc. **33**, 183 (1962). See also J. M. Bowman, J. Phys. Chem. **90**, 3492 (1986).

[12] B. Kendrick and R. T Pack, Chem. Phys. Letters **235**, 291 (1995).

[13] W. H. Miller, J. Phys. Chem. **99**, 12387 (1995).

[14] V. A. Mandelshtam, H. S. Taylor, and W. H. Miller, J. Chem. Phys. **105**, 496 (1996).

[15] R. E. Roberts, R. B. Bernstein, and C. F. Curtiss, Chem. Phys. Letters **2**, 366 (1968) and J. Chem. Phys. **50**, 5163 (1969); R. E. Roberts and R. B. Bernstein, Chem. Phys. Letters **6**, 282 (1970).

[16] D. L. Bunker, J. Chem. Phys. **32**, 1001 (1960); E. L. Knuth, *ibid.* **66**, 3515 (1977).

[17] See, for example, J. S. Shyu, J. Chinese Chem. Soc. **39**, 27 (1992) and **42**, 907 (1995).

[18] R. G. Gilbert and S. C. Smith, *Theory of Unimolecular and Recombination Reactions* (Blackwell, Oxford, 1990); T. Baer and W. L. Hase, *Unimolecular Reaction Dynamics: Theory and Experiments* (Oxford U. Press, New York, 1996).

[19] G. W. Castellan, *Physical Chemistry*, (Addison-Wesley, Reading, MA, 1983), pp. 815, 850-1.

[20] See, for examples, R. A. Alberty, *Physical Chemistry* 6th ed. (Wiley, New York, 1983); P. W. Atkins, *Physical Chemistry* 4th ed. (W. H. Freeman, New York, 1990); J. E. Nicholas, *Chemical Kinetics* (Harper and Row, London, 1976); J. I. Steinfeld, J. S. Francisco, and W. L. Hase, *Chemical Kinetics and Dynamics* (Prentice-Hall, Englewood Cliffs, NJ, 1989); and W. J. Moore, *Physical Chemistry* 4th ed. (Prentice-Hall, Englewood Cliffs, NJ, 1972).

[21] See, for examples, G. G. Hammes, *Principles of Chemical Kinetics* (Academic, New York, 1978); and J. W. Moore and R. G. Pearson, *Kinetics and Mechanism* 3rd ed. (Wiley, New York, 1981).

[22] M. Quack and S. Jans-Bürli, *Molekulare Thermodynamik und Kinetik* (Verlag der

Fachvereine an den Schweizerischen Hochschulen und Techniken, Zürich, 1986), p. 43.

[23] R. E. Roberts, J. Chem. Phys. **54**, 1422 (1971); M. Menzinger, Chem. Phys. Letters **10**, 507 (1971).

[24] L. P. Walkauskas and F. Kaufman, J. Chem. Phys. **64**, 3885 (1976); D. N. Mitchell and D. J. LeRoy, *ibid.* **67**, 1042 (1977).

[25] See, for example, J. Troe, *Physical Chem.: An Advanced Treatise* **6B**, 835 (1975).

[26] See, for example, H. Hippler, K. Luther, A. R. Ravishankara, and J. Troe, Z. Phys. Chem. Neue Folge **142**, 1 (1984).

[27] C. E. Klots, J. Chem. Phys. **53**, 1616 (1970).

[28] B. Otto, J. Schroeder, and J. Troe, J. Chem. Phys. **81**, 202 (1984); H Hippler, V. Schubert, and J. Troe, *ibid.* **81**, 3931 (1984); T.-T. Song, Y.-S. Hwang, and T.-M. Su, J. Phys. Chem. **101**, 3860 (1997).

[29] See, for example, C. J. Cobos, H. Hippler, and J. Troe, J. Phys. Chem. **89**, 342 (1985); R. Forster, M. Frost, D. Fulle, H. F. Hamann, H. Hippler, A. Schlepegrell and J. Troe, J. Chem. Phys. **103**, 2949 (1995); and S. Baer, H. Hippler, R. Rahn, M. Siefke, N. Seitzinger and J. Troe, *ibid.*, **95**, 6463 (1991).

[30] R. J. Duchovic, J. D. Pettigrew, B. Walling, and T. Shipchandler, J. Chem. Phys. **105**, 10367 (1996).

[31] R. T Pack, R. B. Walker, and B. K. Kendrick, Chem. Phys. Letters **276**, 255 (1997).

[32] See, for example, D. L. Martin, L. M. Raff, and D. L. Thompson, J. Chem. Phys. **92**, 5311 (1990) and references therein.

[33] See K. Haug, D. G. Truhlar, and N. C. Blais, J. Chem. Phys. **86**, 2697 (1987) and **96**, 5556 (1992); S. Kumar and N. Sathyamurthy, Chem. Phys. **137**, 25 (1989).

[34] D. W. Schwenke, J. Chem. Phys. **89**, 2076 (1988) and Theor. Chim. Acta **74**, 381 (1988).

[35] D. W. Schwenke, J. Chem. Phys. **92**, 7267 (1990).

[36] J. C. Keck and G. Carrier, J. Chem. Phys. **43**, 2284 (1965).

[37] T. Ashton, D. L. S. McElwain, and H.O. Pritchard, Can. J. Chem. **51**, 237 (1973); H. O. Pritchard, Specialist Periodical Reports, Reaction Kinetics (Chem. Soc., London) **1**, 243 (1975); A. W. Yau and H. O. Pritchard, J. Phys. Chem. **83**, 134 (1979).

[38] R. T. V. Kung and J. B. Anderson, J. Chem. Phys. **60**, 3731(1974).

[39] J. E. Dove and S. Raynor, Chem. Phys. **28**, 113 (1978); J. Phys. Chem. **83**, 127 (1979); and *Complex Chemistry of Reacting Systems*, Springer Ser. Chem. Phys. **47**, 90 (1987).

[40] J. E. Russell and J. S. Shyu, J. Chem. Phys. **91**, 1015 (1989).

[41] See, for example, J. Manz and J. Römelt, Chem. Phys. Letters **77**, 172 (1981); J. Römelt, *ibid.* **150**, 92 (1988); J. A. Kaye and A. Kuppermann, *ibid.* **78**, 546 (1981); **115**, 158 (1985); and **125**, 279 (1988).

[42] M. I. Haftel and T. K. Lim, Chem. Phys. Letters **89**, 31 (1982); J. Chem. Phys. **77**, 4515 (1982) and **84**, 4407 (1986).

[43] H. T. C. Stoof, B. J. Verhaar, and L. P. H. deGoey, Phys. Rev. B **40**, 9176 (1989); P. O. Fedichev, M. W. Reynolds, and G. V. Shlyapnikov, Phys. Rev. Letters **77**, 2921 (1996).

[44] J. M. Greben, A. W. Thomas, and A. J. Berlinsky, Can. J. Phys. **59**, 945 (1981)

[45] A. K. Motovilov, S. A. Sofianos and E. A. Kolganova, Chem. Phys. Letters **275**, 168 (1997).

[46] K. Sakai, Chem. Phys. **220**, 115 (1997).

[47] W. H. Miller, Disc. Faraday Soc. (in press).

[48] J. Qi and J. M. Bowman, J. Phys. Chem. **100**, 15165 (1996) and Chem. Phys. Letters

276, 371 (1997).

[49] See R. T Pack and G. A. Parker, J. Chem. Phys. **87**, 3888 (1987), **90**, 3511 (1989) and references therein.

[50] B. Pan and J. M. Bowman, J. Chem. Phys. **103**, 9661 (1995).

[51] K. Nobusada and K. Sakimoto, Chem. Phys. **197**, 147 (1995).

[52] See G. A. Parker and R. T Pack, J. Chem. Phys. **68**, 1585 (1978) and references therein.

[53] G. A. Pfeffer, J. Phys. Chem. **89**, 1131 (1985).

[54] K. Sakimoto, J. Phys. B **30**, 3881 (1997) and Chem. Phys. **00**, 0000 (1998) (in press).

[55] R. T Pack, R. B. Walker, and B. K. Kendrick, J. Chem. Phys. **00**, 0000 (1998), following paper.

[56] G. W. Wei, S. Alavi, and R. F. Snider, J. Chem. Phys. **106**, 1463 (1997).

[57] R. A. Aziz and M. J. Slaman, Chem. Phys. **130**, 187 (1989).

[58] See, for example, R. D. Levine, *Quantum Mechanics of Molecular Rate Processes* (Oxford U. Press, London, 1969), p. 234, and references therein.

[59] W. J. Meath and R. A. Aziz, Mol. Phys. **52**, 225 (1984).

[60] K. T. Tang and J. P. Toennies, Chem. Phys. **156**, 413 (1991).

[61] N. Levinson, Kgl. Danske Vid. Selskab. Mat-Fys. Medd. **25**, No. 9 (1949).

[62] B. R. Johnson, J. Chem. Phys. **67**, 4086 (1977).

[63] R. B. Walker and E. F. Hayes, J. Chem. Phys. **91**, 4106 (1990).

[64] B. Kendrick and R. T Pack, J. Chem. Phys. **104**, 7502 (1996).

[65] R. T Pack, J. Chem. Phys. **60**, 633 (1974).

TABLES

TABLE I. Properties of the long-lived states of $^{18}Ne_2$

state	(v,j)	ϵ/k_B (K)	τ_{max}(psec)	Γ/k_B (K)	τ_e(psec)	τ_{pass}(psec)	Type
1	(0,0)	-23.56	∞	0	∞	–	bound
2	(0,2)	-22.08	∞	0	∞	–	bound
3	(0,4)	-18.65	∞	0	∞	–	bound
4	(0,6)	-13.33	∞	0	∞	–	bound
5	(0,8)	-6.23	∞	0	∞	–	bound
6	(1,0)	-3.63	∞	0	∞	–	bound
7	(1,2)	-2.72	∞	0	∞	–	bound
8	(1,4)	-0.69	∞	0	∞	–	bound
9	(κ,2)	0.12	36.24	0.20	9.06	196.9	BS
10	(κ,4)	0.48	5.02	0.65	1.26	98.7	BS
11	(1,6)	1.98	78.18	0.39	19.55	13.3	QB
12	(κ,8)	5.33	9.64	3.17	2.41	11.6	BAB
13	(0,10)	2.44	5.2×10^6	5.9×10^{-6}	1.3×10^6	4.4	QB
14	(κ,10)	9.48	3.01	10.17	0.75	9.7	BAB
15	(0,12)	12.15	95.62	0.32	23.91	2.1	QB
16	(κ,14)	22.76	10.55	2.90	2.64	3.1	BAB
17	(κ,16)	34.98	3.77	8.10	0.94	2.9	BAB
18	(κ,18)	48.95	1.92	15.90	0.48	2.7	BAB

TABLE II. Cross Sections (a_0^2) at E/k_B = 30 K from all bound states i=(v,j) into the quasi-bound (0,10) resonant state treated as a scattering (s) or bound (b) state.

f←i	(0,0)	(0,2)	(0,4)	(0,6)	(0,8)	(1,0)	(1,2)	(1,4)
(0,10)(s)←i	0.42	0.98	4.14	16.98	48.29	0.19	0.43	1.02
(0,10)(b)←i	0.42	0.97	4.10	16.83	47.85	0.19	0.43	1.02

TABLE III. Cross Sections (a_0^2) at E/k_B = 30 K from states i=(v,j) into states f=(v',j')

f←i	(0,0)	(0,2)	(0,4)	(0,6)	(0,8)	(1,0)	(1,2)	(1,4)	(1,6)	(0,10)	(0,12)
(0,0)	360.08	19.07	4.59	.78	.12	.89	.15	.01	.00	.02	.00
(0,2)	95.34	398.97	34.93	8.52	1.49	.76	1.16	.27	.02	.23	.04
(0,4)	41.33	62.87	392.92	37.03	9.69	.56	.66	1.08	.19	1.76	.24
(0,6)	10.12	22.14	53.48	391.07	38.30	.76	.66	.60	.66	10.42	1.78
(0,8)	1.97	5.08	18.30	50.09	389.93	.44	.68	.78	.48	38.74	10.06
(1,0)	.89	.15	.06	.06	.03	360.71	15.16	5.51	1.34	.01	.00
(1,2)	.75	1.16	.37	.25	.20	75.82	398.08	32.02	8.84	.10	.05
(1,4)	.12	.48	1.08	.42	.41	49.62	57.63	396.47	27.00	.44	.36
(1,6)	.06	.06	.28	.66	.36	17.38	22.98	39.01	402.05	.61	1.12
(0,10)	.42	.97	4.10	16.83	47.85	.19	.43	1.02	.98	388.64	36.11
(0,12)	.09	.18	.68	3.42	14.79	.09	.26	1.01	2.15	42.99	386.95
(κ,0)	.62	.08	.04	.02	.00	4.55	1.67	.77	1.13	.00	.01
(κ,2)	.44	.88	.21	.12	.05	9.28	9.04	5.47	6.98	.02	.06
(κ,4)	.18	.41	1.06	.30	.22	6.49	9.00	11.97	14.03	.10	.13
(κ,6)	.18	.15	.58	1.58	.58	7.56	11.26	15.59	.00	.59	.55
(κ,8)	.10	.11	.18	1.06	2.56	8.62	14.37	28.72	54.31	1.62	3.73
(κ,10)	.04	.07	.12	.40	1.78	2.63	4.83	12.49	29.11	3.46	5.22
(κ,12)	.03	.05	.13	.41	1.59	.78	1.40	4.05	13.40	4.37	.00
(κ,14)	.04	.06	.19	.77	3.94	.29	.54	1.82	7.48	17.24	48.38
(κ,16)	.01	.02	.05	.16	.75	.10	.19	.67	3.53	4.21	19.06
(κ,18)	.00	.00	.01	.02	.08	.03	.06	.26	1.70	.57	4.83
(κ,20)	.00	.00	.00	.00	.00	.01	.02	.09	.83	.03	.74

TABLE IV. Total cross sections (a_0^2) for possible processes of a given type at E/k_B = 30 K from states i=(v,j).

f←i	(0,0)	(0,2)	(0,4)	(0,6)	(0,8)	(1,0)	(1,2)	(1,4)
i←i	360.08	398.97	392.92	391.07	389.93	360.71	398.08	396.47
b←i	150.52	110.96	112.81	97.14	50.24	128.85	76.11	40.27
QB←i	.57	1.21	5.06	20.90	63.01	17.66	23.66	41.03
BAB←i	.40	.47	1.25	4.38	11.29	20.02	32.67	63.69
3B←i	1.24	1.37	1.31	.44	.27	20.31	19.71	18.21
tot(sum)←i	512.82	512.98	513.34	513.92	514.74	547.54	550.24	559.67
tot(com)←i	512.90	513.07	513.48	514.24	515.58	549.41	552.52	563.39

FIGURES

FIG. 1. Effective potentials (in Kelvin) versus r (in atomic units) for $^{18}Ne_2$ with some bound and continuum wavefunctions, plotted about their energies (ϵ), superimposed on them. The dotted line marks the energy zero. (a) $j = 2$. The maximum amplitude of the resonant wavefunction is at large r. (b) $j = 6$. The energy of the QB wavefunction is barely below the top of the barrier, so that it is only a little localized. (c) The BAB resonant wavefunction for $j = 14$. There is only a little enhancement of the amplitude at small r. See text for discussion.

FIG. 2. 3D perspective plot of the Ne_2 scattering wavefunctions versus distance and energy (ϵ). See text for discussion.

FIG. 3. Collision lifetime (delay time) (in picoseconds) versus Energy ϵ (in Kelvin) of the continuum states of Ne_2 with $j = 4$. At this angular momentum there is a barrier slowing (BS) resonance at low energy, and τ is negative (nonresonant) at all higher energies.

FIG. 4. $d\sigma/d\kappa$ versus κ (atomic units). The integral of each curve gives its integral bound-free cross section, so that this plot gives the contribution from a given energy of relative motion of the Ne atoms. The symbols on the curves label the initial states, i=(v,j): solid circles, (0,0); asterisks, (0,2); solid squares, (0,4); solid triangles, (0,6); X, (0,8); open triangles, (1,0); Y, (1,2); and diamonds, (1,4). (a) $j_f = 0$. These contributions are all due to direct, nonresonant three-body collisions. (b) $j_f = 4$. These contributions are also from the direct, nonresonant 3B continuum. (c) $j_f = 6$. The sharp peaks are from the (1,6) QB state; the broad tail is from the nonresonant 3B continuum. (d) $j_f = 8$. This is mostly due to a BAB resonance. (e) $j_f = 12$. The sharp peaks are from the (0,12) QB state. (f) $j_f = 14$, (g) $j_f = 16$, and (h) $j_f = 18$ are all due to BAB resonances and nonresonant 3B scattering. See text for discussion.

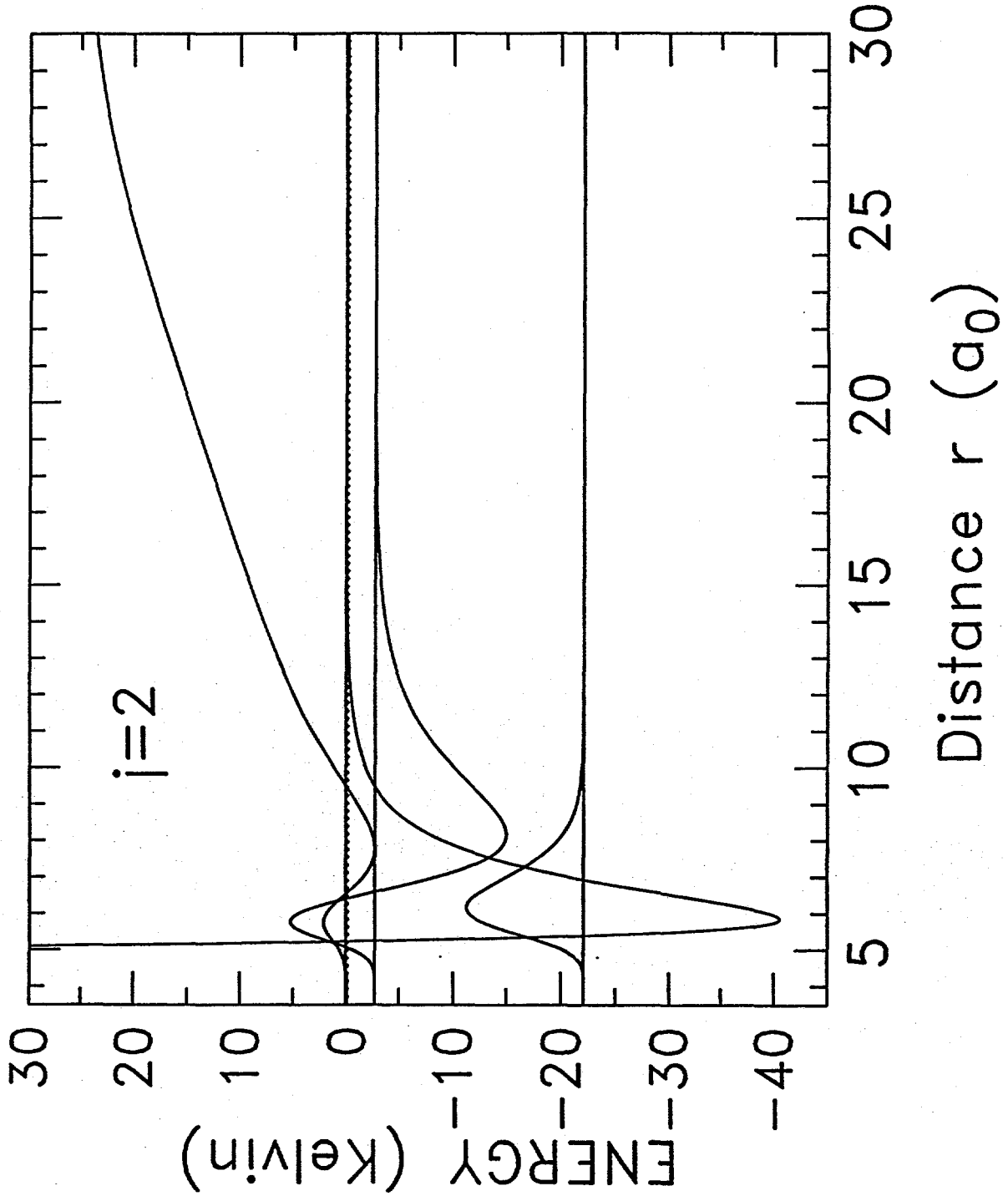
ENERGY (Kelvin)
30
20
10
0
−10
−20
−30
−40
5
10
15
20
25
30
Distance r (a0)
i=2

Figure 1(a)

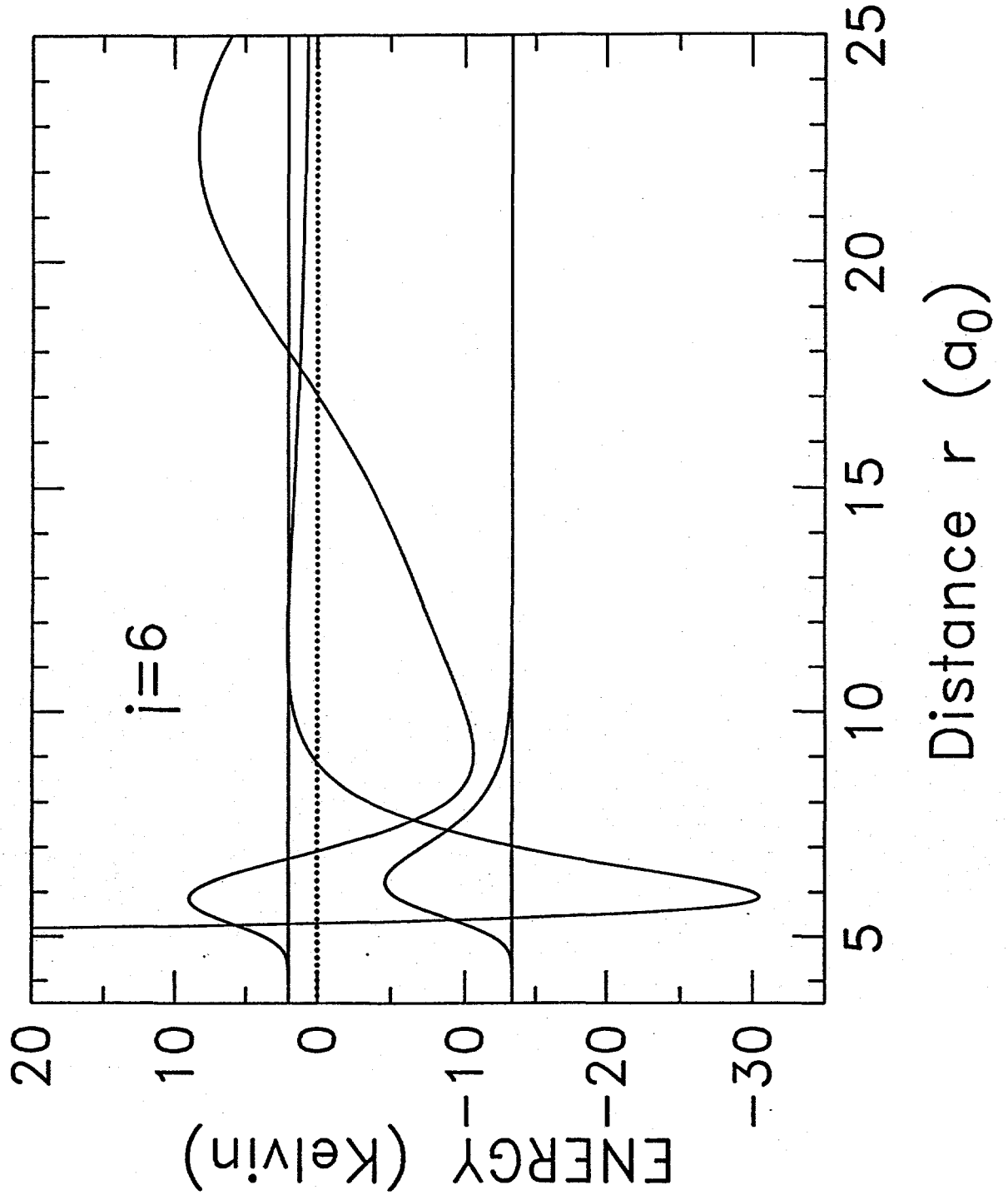

Figure 1(b)

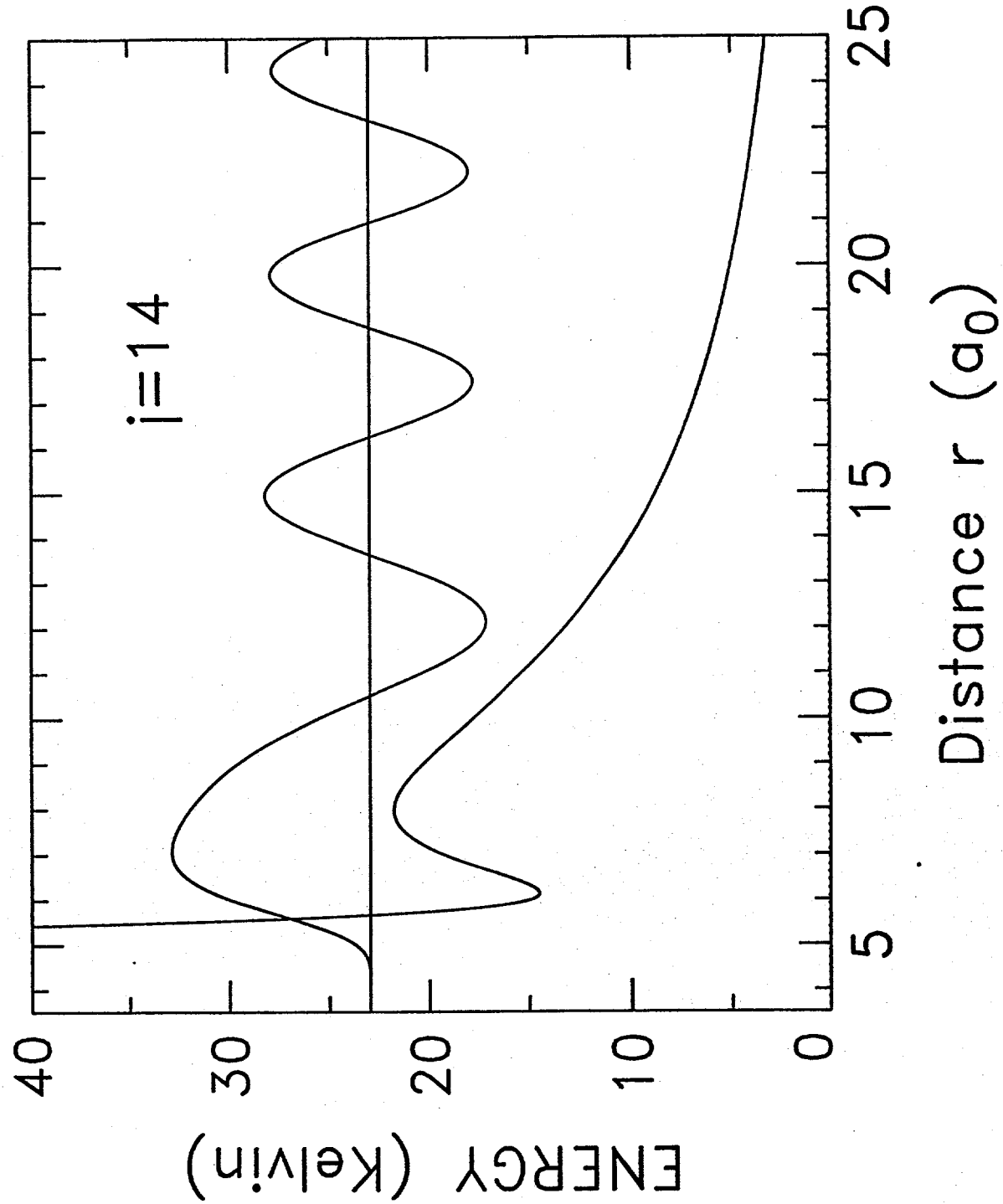

Figure 1(c)

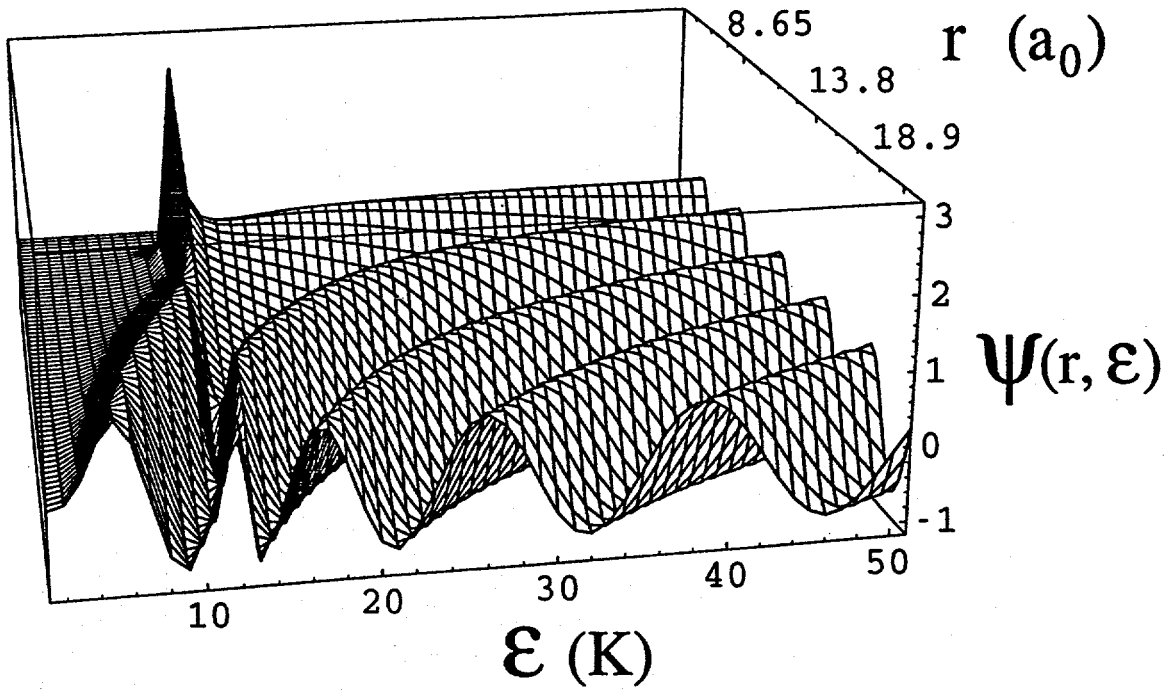

Figure 2

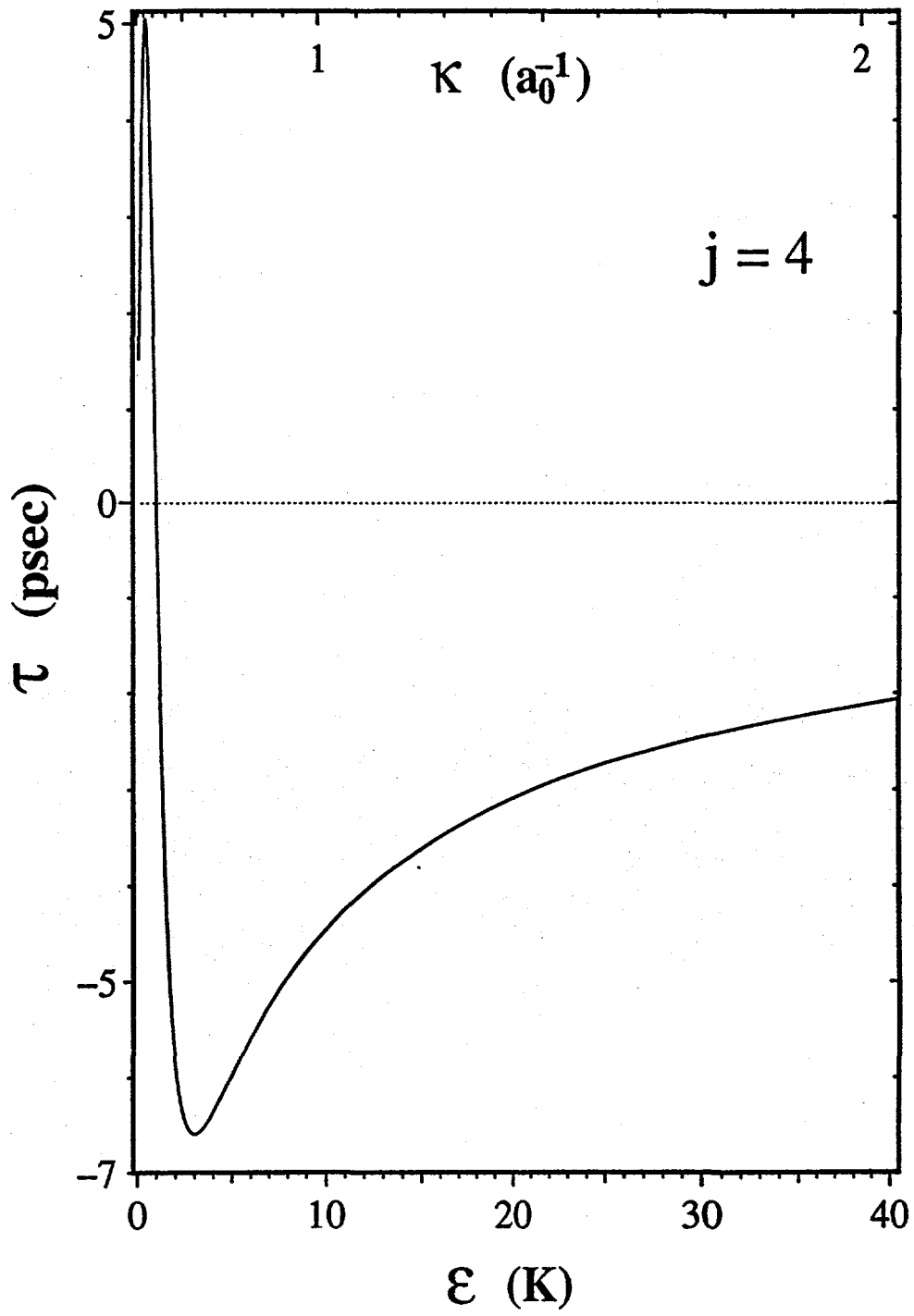

Figure 3

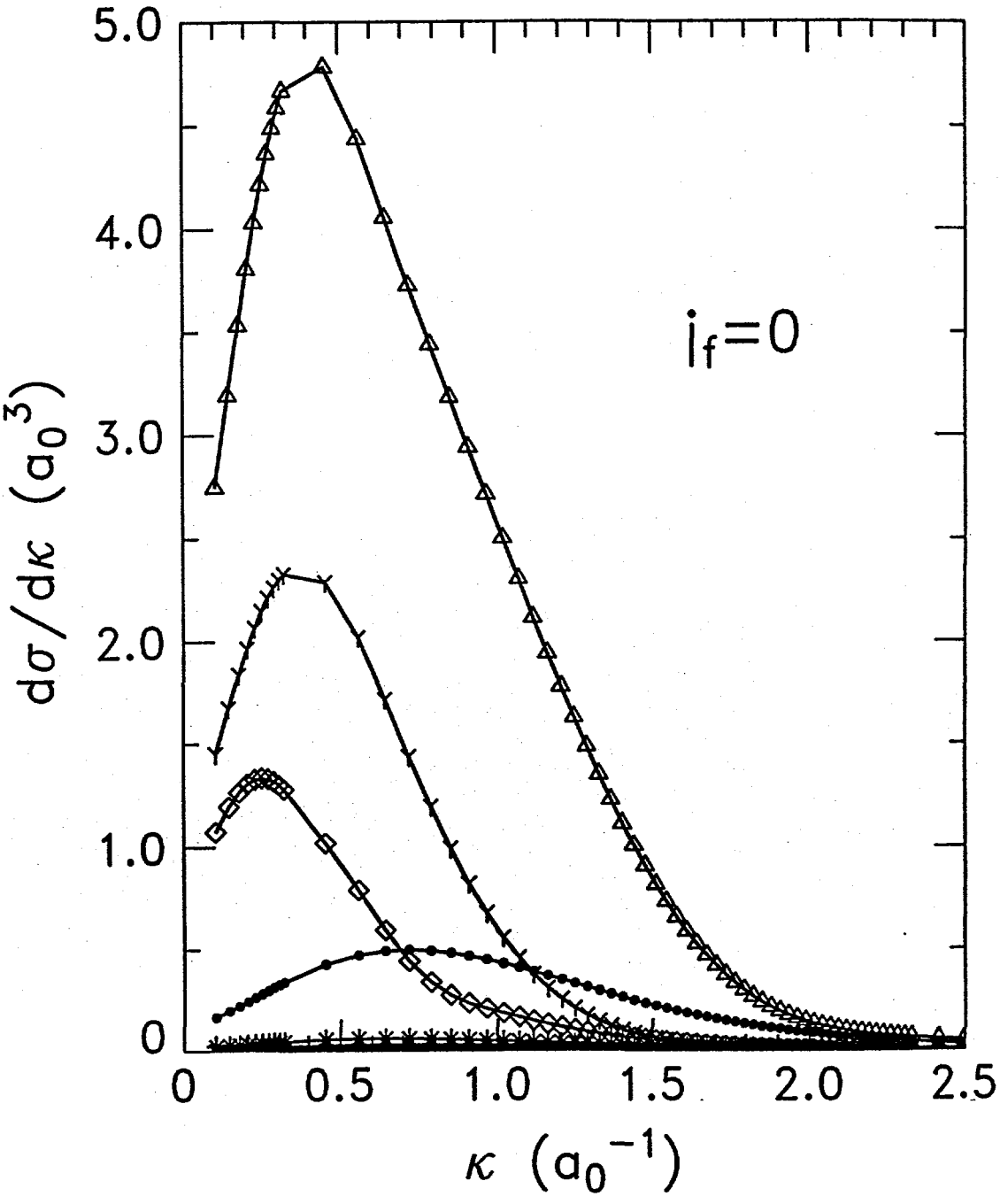

Figure 4(a)

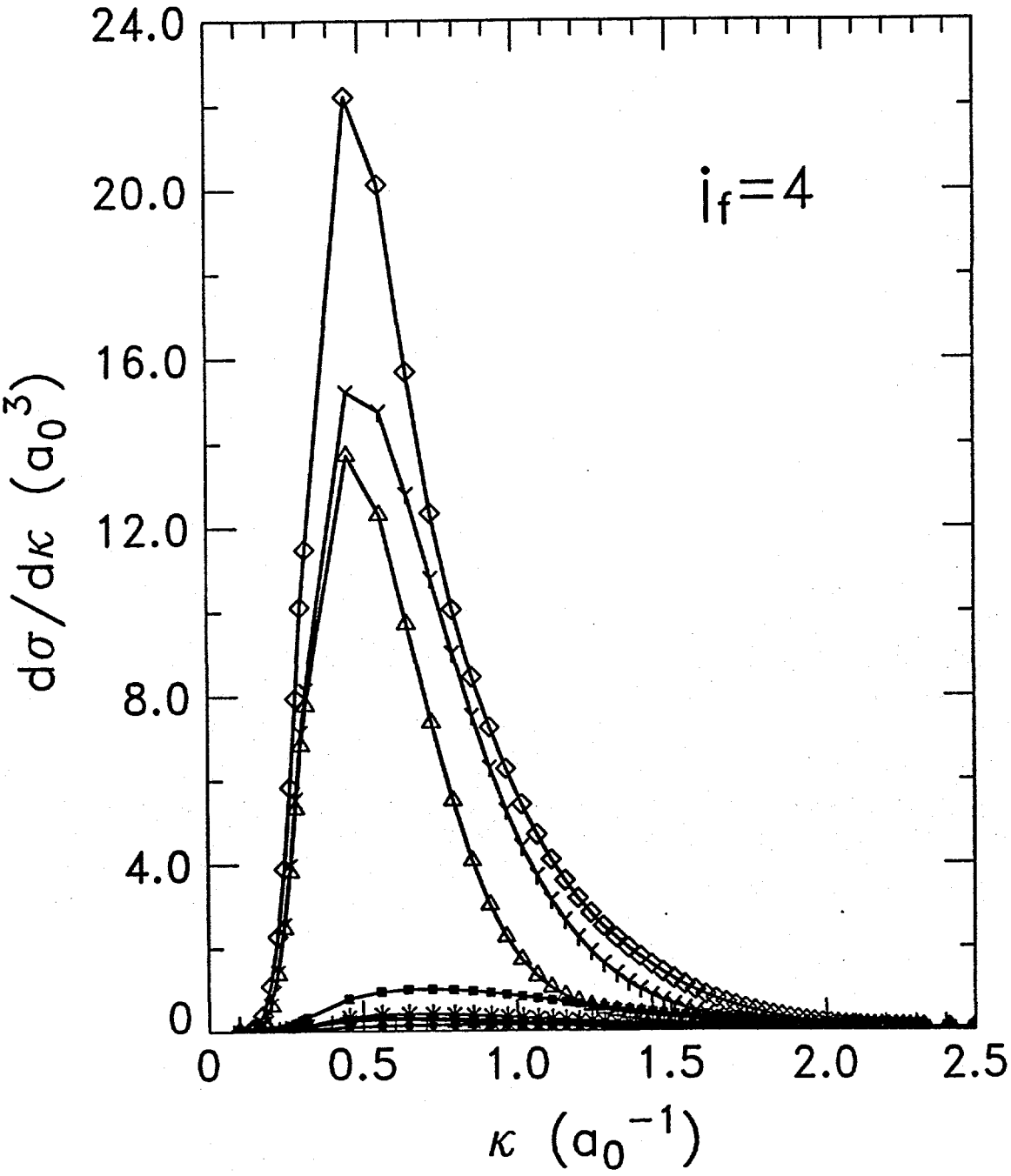
24.0
20.0
16.0
12.0
8.0
4.0
0
0
0.5
1.0
1.5
2.0
2.5
$i_f=4$
$d\sigma/d\kappa\ (a_0^3)$
$\kappa\ (a_0^{-1})$

Figure 4(b)

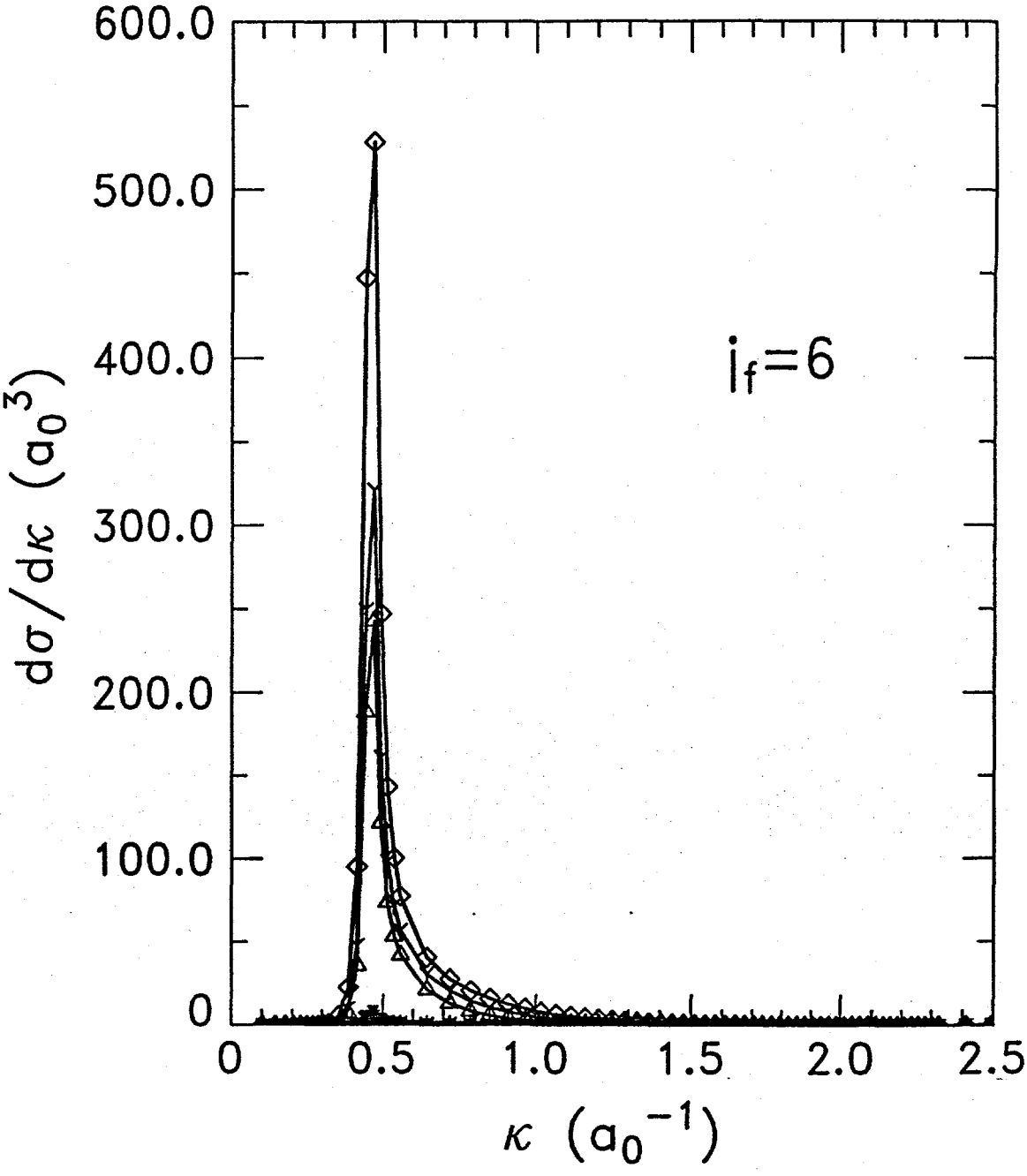
600.0
500.0
400.0
300.0
200.0
100.0
0
0
0.5
1.0
1.5
2.0
2.5
$d\sigma/d\kappa\ (a_0^3)$
$\kappa\ (a_0^{-1})$
$j_f=6$

Figure 4(c)

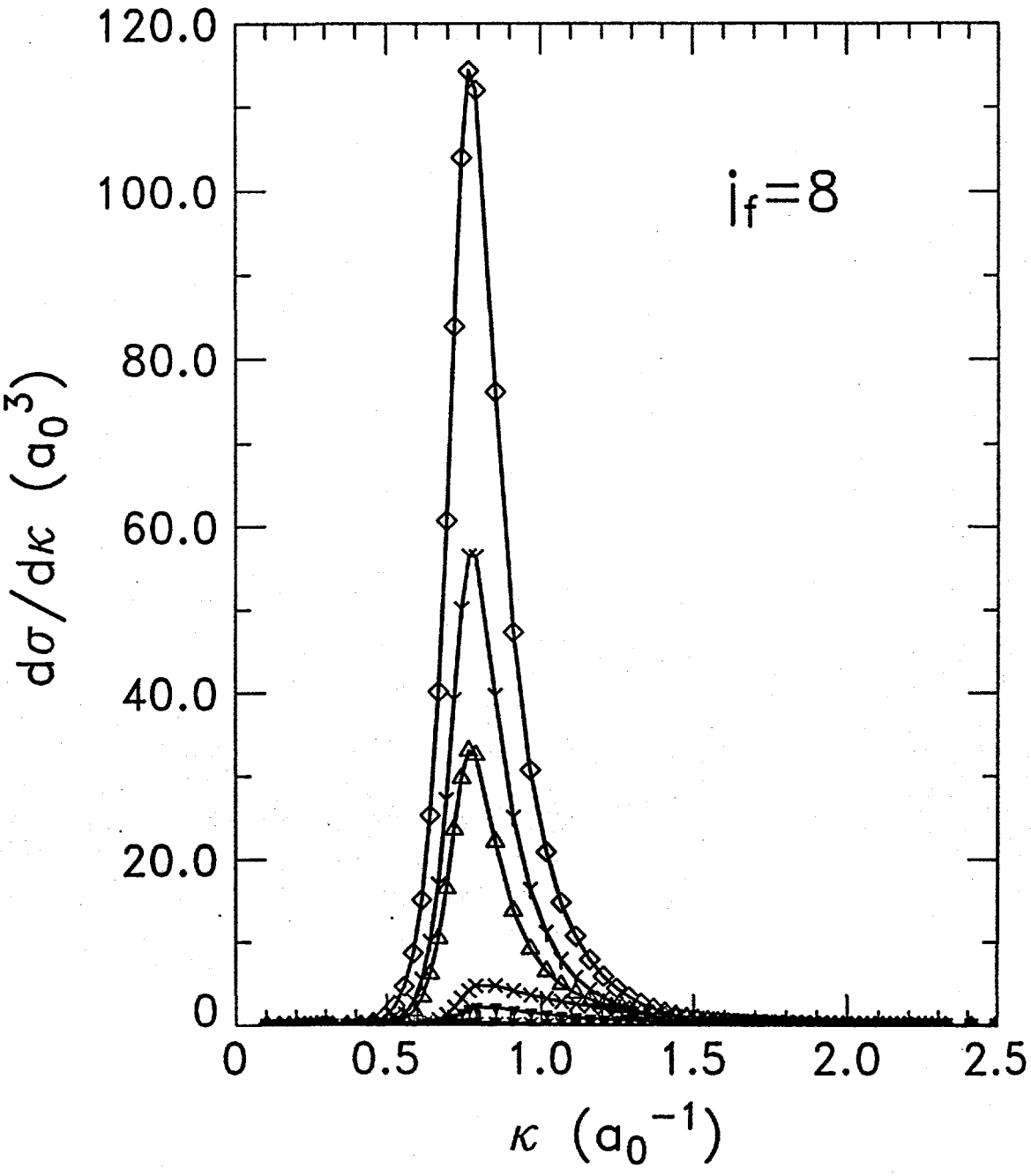
120.0
100.0
80.0
60.0
40.0
20.0
0
0
0.5
1.0
1.5
2.0
2.5
$j_f=8$
$d\sigma/d\kappa\ (a_0^3)$
$\kappa\ (a_0^{-1})$

Figure 4(d)

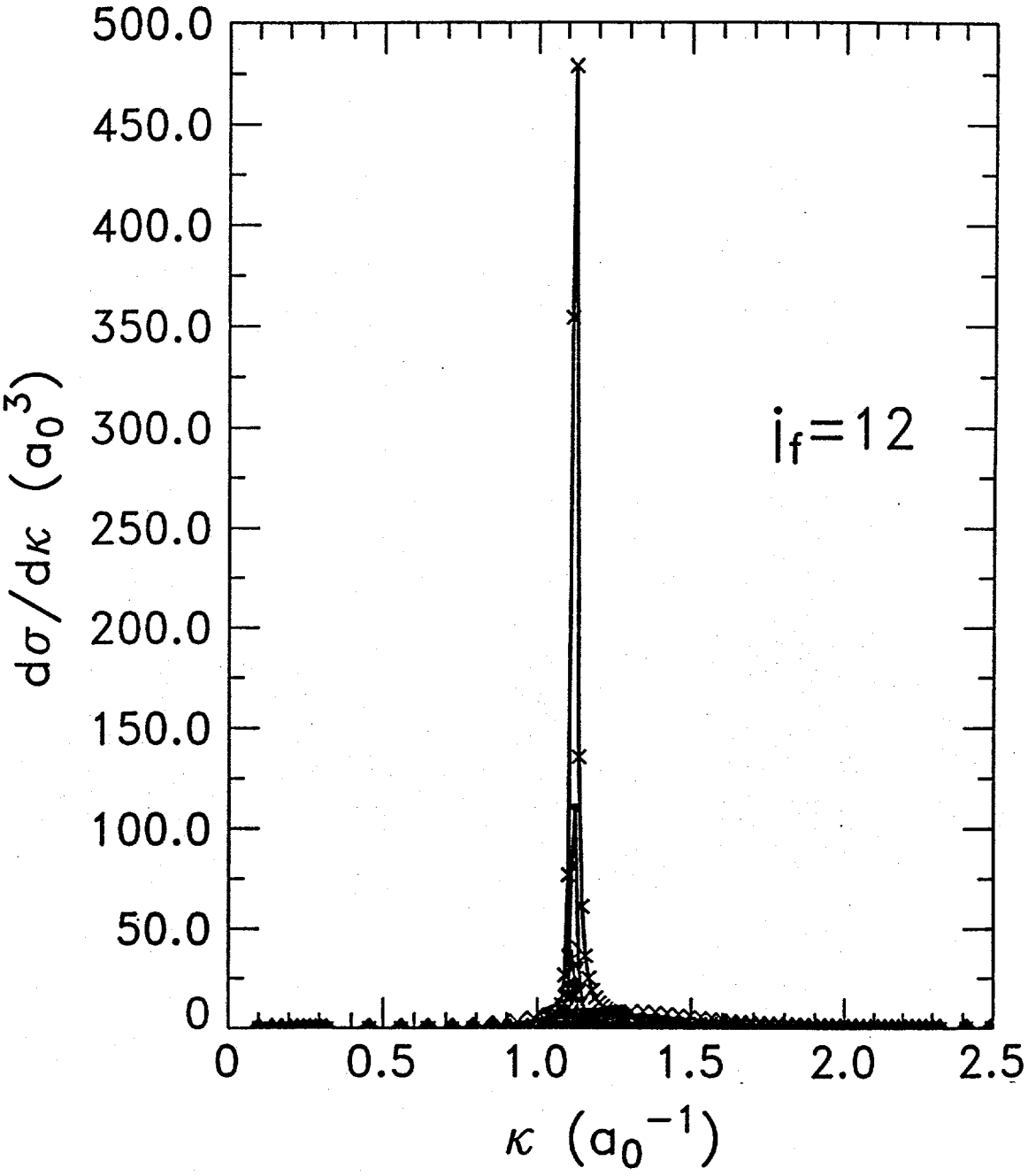
500.0
450.0
400.0
350.0
300.0
250.0
200.0
150.0
100.0
50.0
0
0
0.5
1.0
1.5
2.0
2.5
dσ/dκ (a0^3)
κ (a0^-1)
lf=12

Figure 4(e)

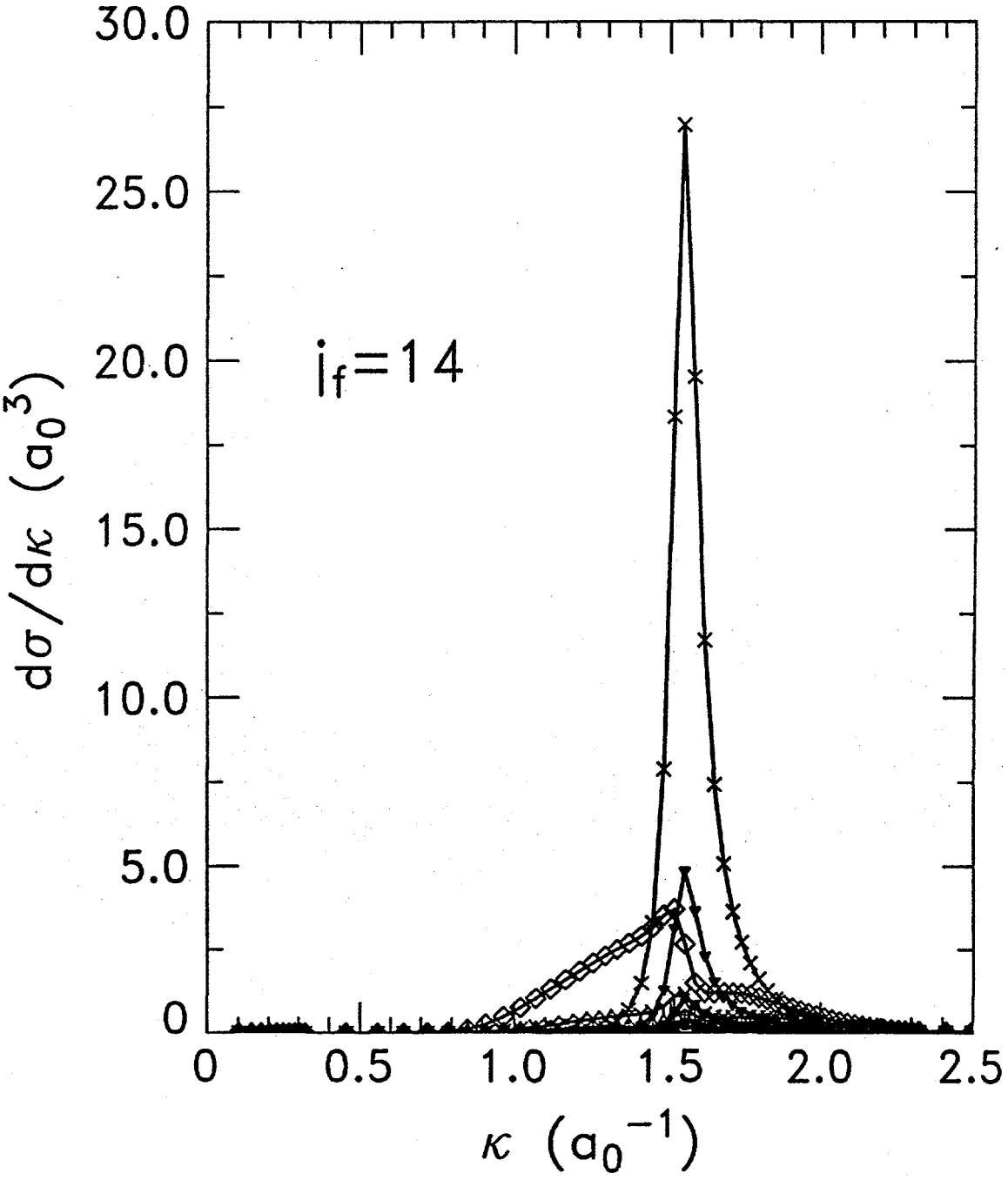
30.0
25.0
20.0
15.0
10.0
5.0
0
$i_f=14$
$d\sigma/d\kappa$ (a_0^3)
0
0.5
1.0
1.5
2.0
2.5
κ (a_0^{-1})

Figure 4(f)

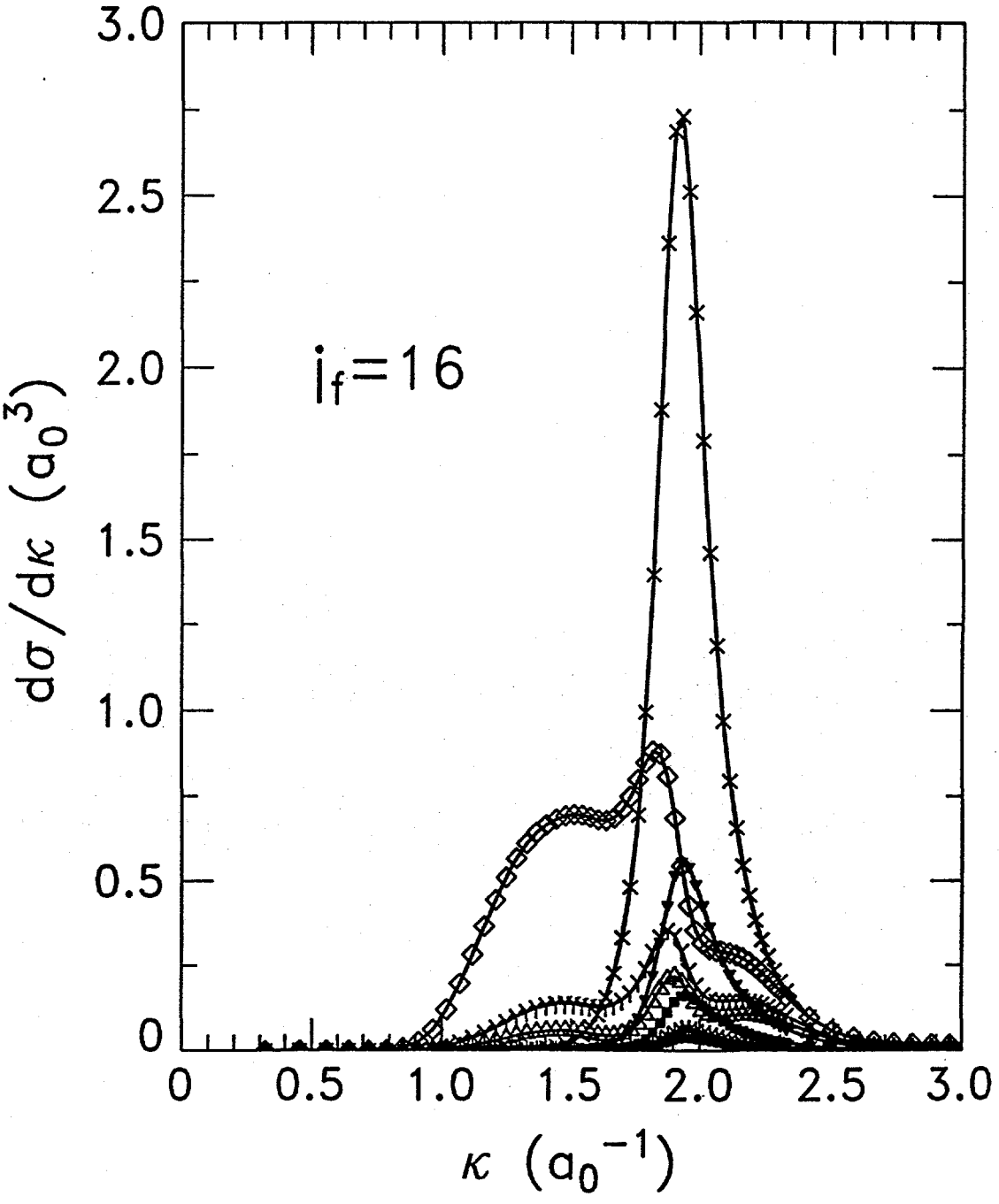
3.0
2.5
2.0
1.5
1.0
0.5
0
$i_f = 16$
$d\sigma/d\kappa$ (a_0^3)
0
0.5
1.0
1.5
2.0
2.5
3.0
κ (a_0^{-1})

Figure 4(g)

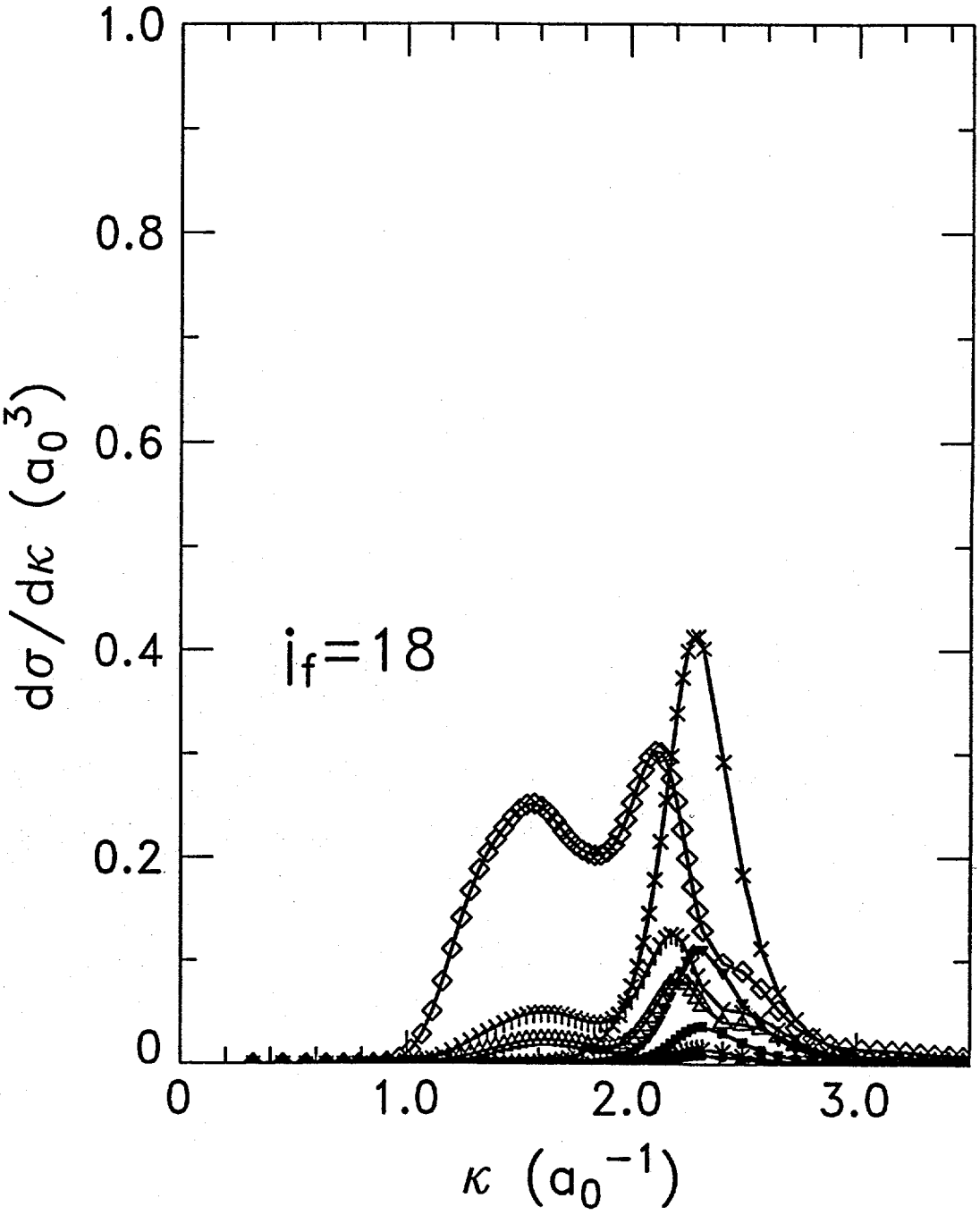

Figure 4(h)